iScience

Article

Tunable universal OR-gated CAR T cells for AML

Graphical abstract

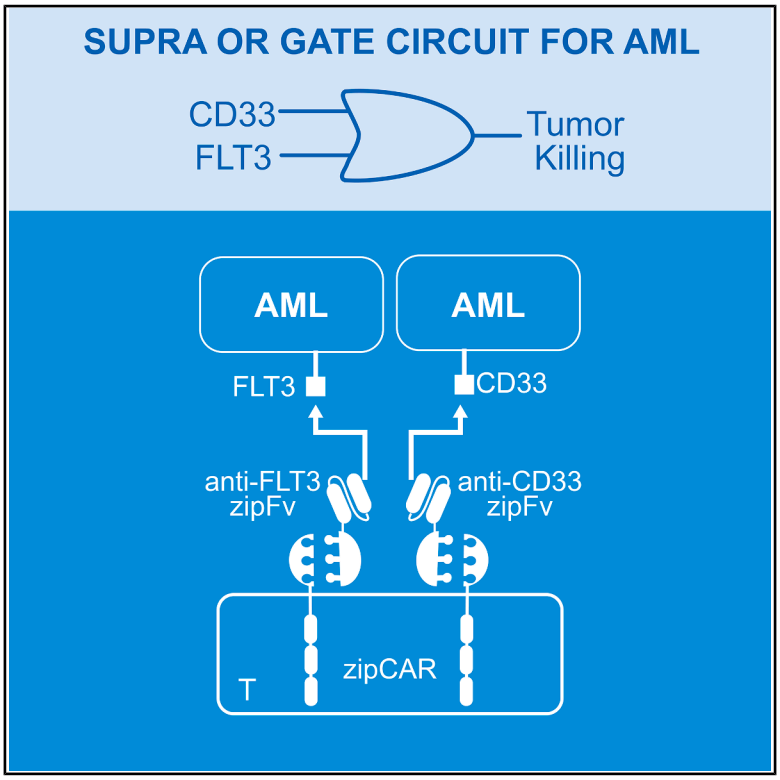

Highlights

- SUPRA OR gate CAR targets multiple AML antigens, such as FLT3 and CD33, simultaneously
- Conveniently tunable CAR activity through variable dosing of the adapter
- Identify a dose range that can discriminate tumor cells from hematopoietic stem cells

Authors

Menna Y. Siddiqui, Jingyao Chen, Joey Zhuoying Huang, ..., Marcela Guzmán Ayala, Nicholas W. Frankel, Wilson W. Wong

Correspondence

wilwong@bu.edu

In brief

cellular therapy; immunology; cancer

Siddiqui et al., 2026, iScience *29*, 117008
August 21, 2026
https://doi.org/10.1016/j.isci.2026.117008

CellPress

iScience

CellPress
OPEN ACCESS

Article

Tunable universal OR-gated CAR T cells for AML

Menna Y. Siddiqui,[1] Jingyao Chen,[1] Joey Zhuoying Huang,[1] Madeline Loffredo,[2] Seunghee Lee,[1] Han Deng,[3] Yongshuai Li,[3] Nelia Leemans,[3] Tim Lu,[3] Brian S. Garrison,[3] Marcela Guzmán Ayala,[3] Nicholas W. Frankel,[3] and Wilson W. Wong[1,4,*]

[1]Department of Biomedical Engineering and Biological Design Center, Boston University, Boston, MA, USA
[2]Department of Materials Science and Engineering, Boston University, Boston, MA, USA
[3]Senti Biosciences, South San Francisco, CA, USA
[4]Lead contact
*Correspondence: wilwong@bu.edu
https://doi.org/10.1016/j.isci.2026.117008

SUMMARY

Acute myeloid leukemia (AML) is characterized by antigen heterogeneity and poor prognosis. Here, to tackle the heterogeneity of AML, we combined FLT3 with CD33 in a combinatorial OR-gate approach using our split, universal, programmable (SUPRA) chimeric antigen receptor (CAR) platform. The split platform affords tunability over activation levels and multiplexed targeting. We characterized the specificity and sensitivity of different SUPRA CAR adapters for each target across a panel of target cell lines. Our results demonstrate that this CAR system can effectively target two antigens with equivalent efficacy to conventional CARs while reducing the engineering burden of designing CAR T cells against multiple antigens. Furthermore, we can characterize an effective dose range where off-target cytotoxicity against hematopoietic stem and progenitor cells is minimized. Our SUPRA OR gate has the potential to provide an effective and safer solution to treating AML.

INTRODUCTION

Acute myeloid leukemia (AML) is a subset of leukemia that begins in the blood-forming cells of the bone marrow, and has a particularly poor prognosis, with a 5-year survival rate of just over 30%.[1–3] Despite advances in conventional treatments such as chemotherapy and stem cell transplantation,[4–8] there is a significant unmet need for new and effective therapies for AML patients.[9,10] Immunotherapy using T cells engineered to target cancer-specific surface antigens has emerged as a promising approach for cancer treatment. Chimeric antigen receptor (CAR) T cell therapy has demonstrated remarkable efficacy against certain hematological malignancies, with six FDA approved clinical products targeting CD19 in B-cell malignancies and BCMA in multiple myeloma.[11–16] Additionally, there are over 500 clinical trials currently underway investigating CAR T cell treatment for other diseases, including AML.[17,18]

CAR T therapy involves genetically modifying a patient's own T cells to express a CAR that recognizes and binds to a specific antigen present on cancer cells. Once the CAR T cells are infused back into the patient, they can selectively target and kill cancer cells, leading to durable and potentially curative responses. However, CAR T therapy for AML has been challenging due to the heterogeneity of this disease—it is characterized by a wide spectrum of mutations that influence the phenotype and disease progression for each individual patient (Figure 1A).[19–21] In addition to clonal heterogeneity, many of the surface antigens shown to be overexpressed in AML are also expressed on healthy hematopoietic stem cells (HSCs), which has made it difficult to find a suitable antigen target for therapy (Figure 1B).[22]

Current CAR T therapies, including many of those in clinical trials, use conventional CAR designs consisting of a fixed, antigen-specific scFv targeting a single cancer antigen coupled with intracellular signaling domains for T cell activation. For B-cell malignancies, CD19 has proven to be an ideal target antigen due to its restricted expression on B-cell lineages and not on other hematopoietic lineages. Since no such single antigen has been identified for AML, conventional CAR designs have shown severe on-target, off-tumor toxicity.[23] Moreover, the heterogeneity of AML makes it difficult for a single-target strategy to achieve a complete response without the risk of refractory disease.

Combinatorial antigen-targeting presents a potentially effective strategy for addressing heterogeneity and off-tumor toxicity. Our group and others have implemented engineered Boolean logic gates, such as "OR," "AND," and "NOT," to advance the targeting capabilities of CAR T cells.[24–33] In particular, OR gate logic can target multiple antigens to prevent antigen escape and subsequent disease relapse due to AML heterogeneity (Figure 1C). Furthermore, by decoupling the antigen-targeting modality from the CAR design, a split CAR design could add an additional layer of safety and tunability not available within other approaches.[34]

To achieve this, we have previously developed a split, universal, and programmable (SUPRA) CAR system composed of a universal chimeric receptor expressed on the T cell, zipCAR,

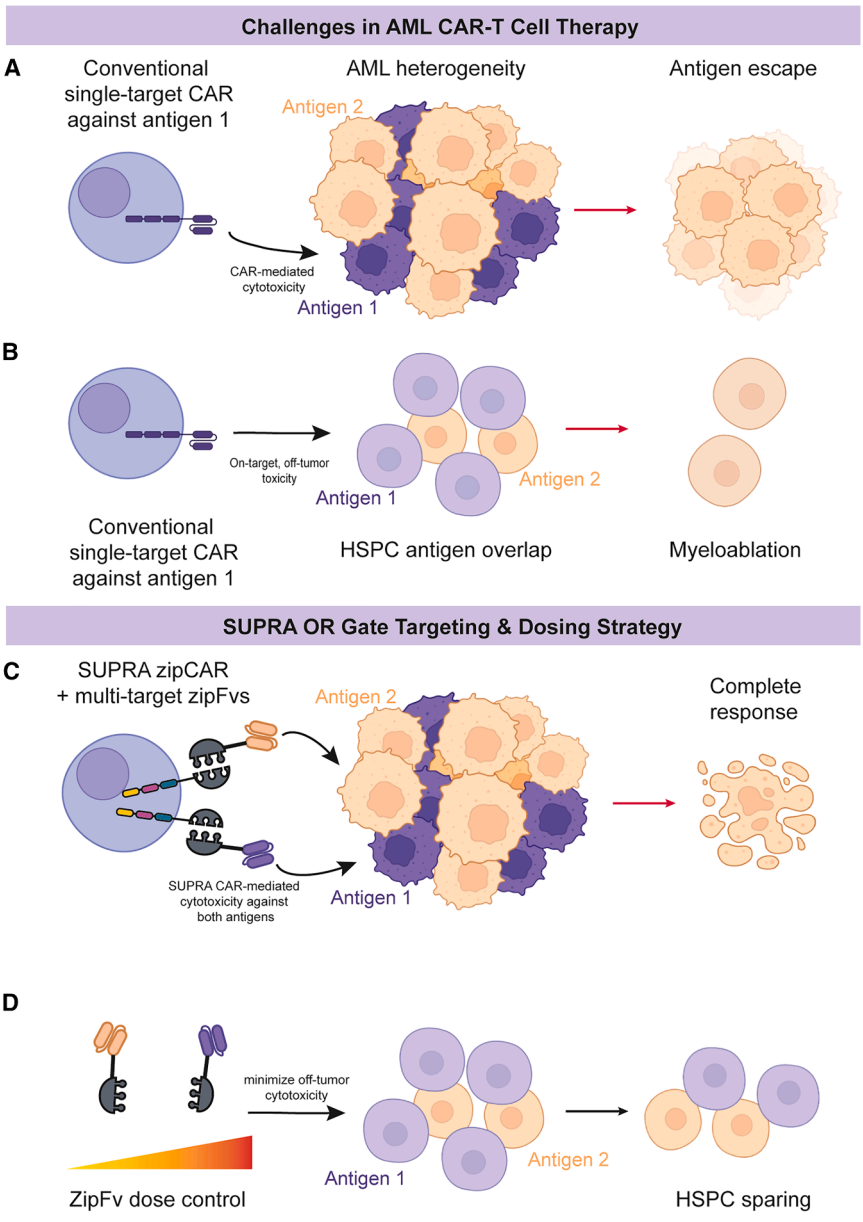

Figure 1. SUPRA can address common challenges in AML CAR-T cell therapy

(A) AML heterogeneity poses a challenge for conventional CAR T therapy against a single target, leading to antigen escape.

(B) Healthy hematopoietic stem cells express many of the same antigens as AML, leading to myeloablation.

(C) By targeting multiple antigens using a SUPRA OR-gate configuration, we can combat antigen escape and approach a complete response.

(D) By optimizing the dosing of zipFv, we can identify a therapeutic dose that spares HSCs while eliminating AML cells.

coupled with a soluble antigen-binding adapter, zipFv, that contains a leucine zipper and scFv.[35] The SUPRA system enables OR gate logic and a tunable T cell response that corresponds to the concentration of each zipFv supplied to the system. We leverage this design to target two AML-associated antigens, CD33 and FLT3, which have been identified as therapeutic targets and are currently being explored in single-target conventional CAR T clinical trials.[23,36,37] Over 80% of AML cases are CD33^{+}, and the first targeted AML therapy introduced was gemtuzumab ozogamicin, a monoclonal anti-CD33 antibody conjugated with an anti-tumor drug.[38,39] However, fatal adverse events such as infection and acute respiratory distress syndrome led to its temporary withdrawal for 7 years before re-approval,[40] and it remains efficacious mainly in patients with very high expression of CD33. Recently, bispecific T cell engagers (BiTEs) and anti-CD33 CAR T designs have been explored in phase I clinical trials,[41,42] with mixed results due to rapid disease progression and the manufacturing challenges of these modalities. Similarly, the FMS-like tyrosine kinase-3 (FLT3) is one of the most frequently mutated genes in AML, accounting for approximately 30% of AML cases.[3,22,43,44] The two main mutation types are an internal tandem duplication (ITD), accounting for approximately 25% of all AML cases, or point mutations in the tyrosine kinase domain (TKD), with a lower incidence of approximately 7%–10% of all cases.[43] The FLT3-ITD mutation has been hypothesized to confer a growth advantage and become the dominant clone at relapse for patients with this mutation present at diagnosis. This mutation has thus been correlated with poor outcomes, and there remains to be an FDA-approved targeted therapy against this antigen. CAR-T designs against FLT3 are being actively explored,[36,45] making it a suitable candidate for our proposed combinatorial approach. Additionally, FLT3-ITD mutations have been correlated with increasingly elevated expression of CD33, especially in certain subtypes of AML such as KMT2A-mutated infant AML, adding to the potential impact of a combinatorial targeting approach.[39,46] By decoupling the targeting modality from the CAR T design, we anticipate that our SUPRA system can alleviate some of the manufacturing challenges of validating new CAR-T therapies while allowing for control over dosing schedules to obtain optimal efficacy for each patient. We show that the relative affinity of each scFv to its target antigen has significant effects on the efficacy of combinatorial dosing, which we have characterized to identify an optimal dose for each target antigen. Additionally, we demonstrate how zipFv dose control can identify a therapeutic window that effectively eliminates tumor cells with varying antigen expression levels while sparing most healthy HSCs (Figure 1D).

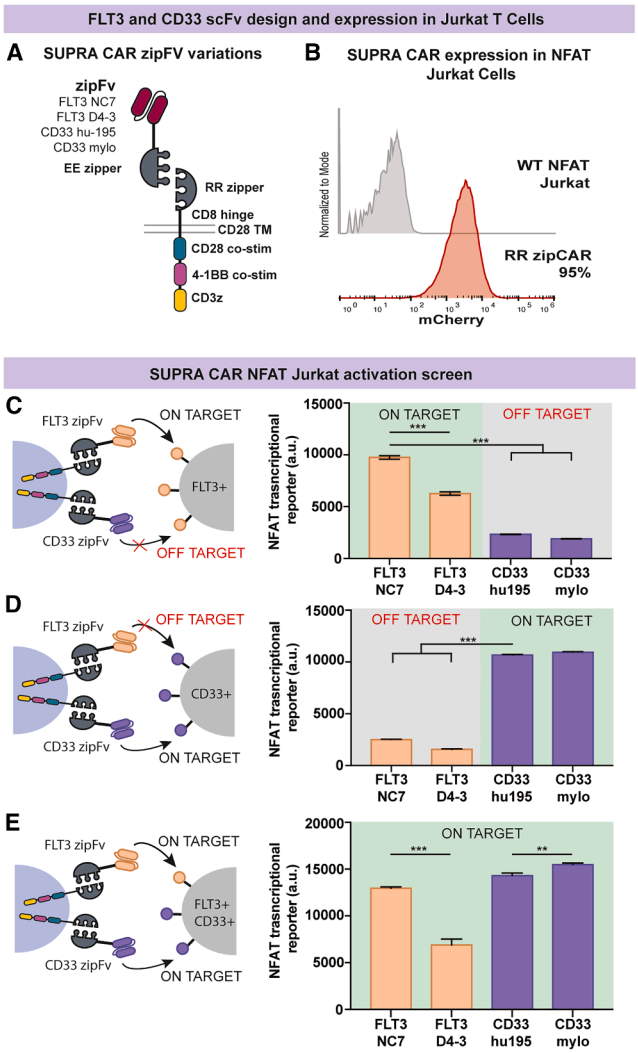

Figure 2. SUPRA CAR OR-Gate against FLT3 and CD33 design and initial activity screening

(A) Four zipFv variations were designed as a fusion of an EE leucine zipper to FLT3 or CD33 scFv clones and paired with a 3rd generation RR CAR containing both CD28 and 4-1BB costimulatory domains in addition to the CD3z activation domain.

(B) RR CAR was transduced into NFAT-GFP Jurkat T cells with a transduction efficiency of 95%.

(C) FLT3+ K562 cells were co-cultured with RR CAR in the presence of either FLT3 zipFv to assess on-target activity or CD33 zipFv to assess off-target activity.

(D) CD33$^+$ K562 cells were co-cultured with RR CAR in the presence of either CD33 zipFv to assess on-target activity or FLT3 zipFv to assess off-target activity.

(E) Double+ CD33$^+$/FLT3+ K562 were co-cultured with RR CAR in the presence of each zipFv variation to assess on-target activity. In all co-culture conditions, an E:T ratio of 1:1 was used, and 50 ng of the corresponding zipFv was added. CAR-T activation is reported as the expression of GFP transcribed downstream of the NFAT reporter. Values shown are the means of technical triplicate samples with error bars indicating +1 standard deviation. Statistical analysis using unpaired two-tailed *t* test was performed. Not significant $p > 0.05$, $^*p < 0.05$, $^{**}p < 0.01$, $^{***}p < 0.001$.

RESULTS

Design and characterization of SUPRA CAR against target antigens FLT3 and CD33

The SUPRA system comprises a universal zipper CAR (zipCAR) and a recombinant protein combining a leucine zipper and an scFv (zipFv). To design zipFvs targeting FLT3 and CD33, we chose two clonal variations of each targeting antibody fragments used in the scFv design: anti-FLT3 (NC7), anti-FLT3 (D4-3), anti-CD33 humanized monoclonal 195 (hu-195), and anti-CD33 Mylotarg (mylo) (Figure 2A). These were fused with an EE zipper through a GS linker and paired with a third-generation RR-CAR in various configurations (Figure S1A). It is important to note that the FLT3 mutations characteristic of FLT+ AML are in internal domains with no reported effect on the extracellular protein structure and binding affinity to scFvs. To characterize the function of these zipFvs, we screened all zipFvs with RR-CAR transduced NFAT-GFP Jurkat T cells (Figure 2B) against engineered CD33$^+$, FLT3+, and FLT3+CD33$^+$ K562 CML target cell lines in *in vitro* co-culture activation assays. Briefly, RR-CAR transduced NFAT GFP cells were co-cultured with target cells at a 1:1 effector to target (E:T) ratio with or without 50 ng of adapter zipFv, and NFAT transcriptional activity was measured via the T cell activation NFAT-GFP transcription reporter expression to assess on-target and off-target activity. This initial testing in Jurkat cells allowed us to quickly screen for binder activity and test a variety of designs in an easy to transduce and maintain cell line. The FT3 NC7 zipFv variant showed significantly higher activation than the D4-3 variant, while both showed higher activation levels than the off-target CD33 zipFvs when targeting FLT3+ K562 (Figure 2C). In contrast, both CD33 zipFv variants had high on-target activity against CD33$^+$ K562 that was significantly higher than off-target activity by FLT3 zipFv variants (Figure 2D). Similar to the results against single positive K562 targets, FLT3 NC7 variant showed significantly higher activity compared to D4-3 against CD33$^+$FLT3+ K562 (Figure 2E). Although the CD33 mylo variant showed slightly higher activity than the hu195 variant against the double+ target cells, the protein production yield of CD33 hu195 zipFv was higher (Figure S1B), leading us to favor this variant over the CD33 mylo zipFv.

In addition to the EE-RR zipper SUPRA design, we also characterized the activity of the SUPRA system generated with FOS leucine zippers, pairing with a JunD zipCAR transduced into NFAT-GFP Jurkat cells (Figure S2A). However, both FLT3 FOS zipFvs show reduced on-target activity that was not significantly higher than the off-target signal (Figure S2B). In contrast, the CD33 FOS zipFv variants showed similarly high on-target activity compared to their EE counterparts (Figure S2C). We additionally designed conventional single-target CAR constructs for each scFv variant (Figure S1A). We transduced these constructs into NFAT-GFP Jurkat T cells to compare their activity against our SUPRA system (Figure S3A). While the activation trends were similar, all conventional designs exhibited lower maximum activation levels against their corresponding single+ targets, resulting in a lower fold change between on-target and off-target states (Figures S3B and S3C). Based on results of these NFAT Jurkat activation assays, the clonal variation FLT3 NC7 outperformed the FLT3 D4-3 clone, and the EE-RR leucine zipper

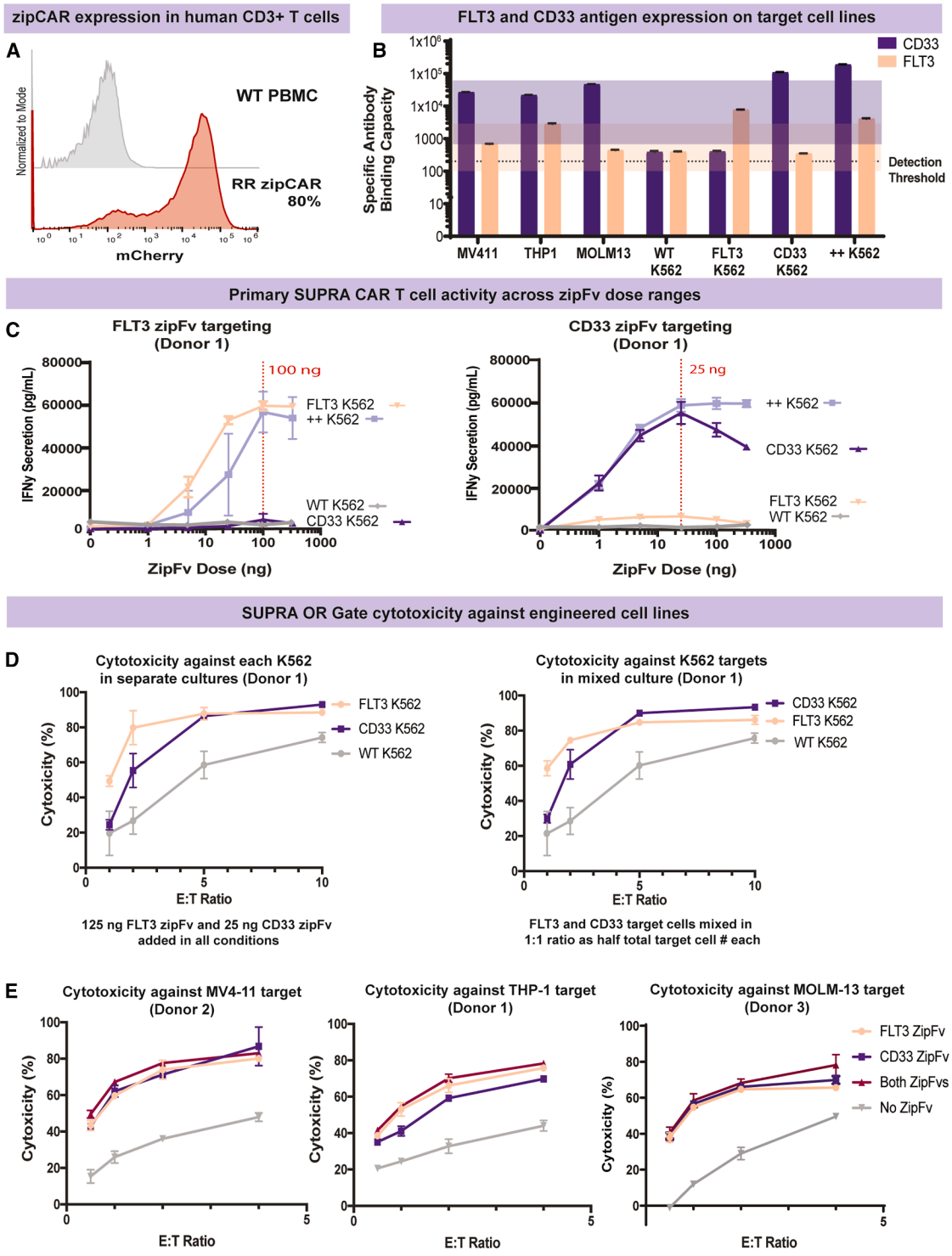

Figure 3. Primary CD3⁺ SUPRA CAR T cell activity and cytotoxicity against AML target cell lines

(A) RR zipCAR was transduced into primary CD3⁺ human T cells with a transduction efficiency of ~80%.

(B) MESF quantitative fluorescence kit from Bangs Laboratories was used to quantify the antibody binding capacity against FLT3 and CD33 antigens on engineered K562 cell lines and MV4-11, THP-1, and MOLM-13 cell lines. The QuickCal pre-formatted template was used to plot the standard curve and determine the detection threshold. Results are plotted as the mean of three technical replicates with error bars indicating +1 standard deviation. Colored bands represent surface expression range in primary human AML samples.

(legend continued on next page)

system outperformed the FOS-JUN leucine zipper pairs for FLT3 targeting. Importantly, protein production yield varied between clonal variations, with FLT3 NC7 and CD33 hu-195 yielding more zipFv protein (Figures S1B and S1C). Thus, we decided to move forward with these two zipFvs and the EE-RR leucine zipper pairs for further characterization of the OR gate.

Primary CD3$^+$ CAR T cell cytotoxicity against AML target cell lines

To assess specific lysis of CD33 and FLT3 expressing target cells, RR-CAR was transduced into primary CD3$^+$ T cells with a transduction efficiency of over 80% for use in *in vitro* co-culture cytotoxicity assays (Figure 3A). As a model for antigen expression heterogeneity, we characterized the antigen expression levels of the engineered K562 CML cell lines, as well as the MV4-11 human AML cell line, MOLM-13 human AML cell line carrying the FLT3-ITD, and THP-1 acute monocytic leukemia cell line, using a standardized fluorochrome-conjugated MESF (molecules of equivalent soluble fluorochrome) bead kit to determine antibody binding capacity against FLT3 and CD33 (Figure 3B). This assay compares fluorescence intensity of the target cell lines stained with a saturating amount of labeled antibody against a mixture of labeled beads with a known quantity of conjugated fluorochrome via flow cytometry to extrapolate the quantity of surface protein. This value is divided by the fluorophore to protein ratio of the staining antibody to determine the specific antibody binding capacity per cell. Prior analyses of primary human AML samples have demonstrated that surface FLT3 expression can range from ~100 to 3000 molecules per cell, with distributions comparable to those observed across commonly used AML cell lines, supporting the clinical relevance of these models.[47] Similarly, CD33 expression has been shown to vary widely in primary AML bone marrow blasts, ranging from ~700 to 60,000 molecules/cell with an average of ~10,000 molecules/cell.[39] These expression ranges are depicted by the colored bands in Figure 3B. Given the range of expression levels observed in our MESF analysis, we determined these cell lines provide an acceptable model to test the functionality of the OR gate, with the engineered K562 cell lines serving as a model of overexpression and the WT K562 cell line serving as a low-expression negative control.

A key feature of the SUPRA system is zipFv dose-dependent activity, which allows us to choose an optimal dose for maximum T cell activation. To identify this dose for each zipFv, primary CD3$^+$ RR-CAR T cells were co-cultured with K562 target cell lines in a 2:1 E:T ratio with varying amounts of zipFv for 24 h, followed by the collection of the supernatant to measure IFNy secretion as an indication of T cell activity. The FLT3 zipFv reached maximum activity at a dose of 100 ng in a 200 μL coculture, with minimal off-target activity against CD33$^+$ and WT K562 cells (Figure 3C). In contrast, the CD33 zipFv saturated activity at a lower dose of 25 ng and exhibited the Hook effect at higher doses against the CD33$^+$ K562 target (Figure 3C). The Hook effect occurs at high concentrations when the excess analyte, in this case the CD33 zipFv, saturates binding on both the target cells and effector. The likelihood of this behavior increases with increased binding affinity of the scFvs against their target antigen, which we further characterize below.

The cytotoxicity against the K562 target cell lines at different E:T ratios was characterized through *in vitro* co-culture cytotoxic assays using a FLT3 zipFv dose of 125 ng and a CD33 zipFv dose of 25 ng in all conditions to ensure that the presence of both zipFvs did not interfere with the lysis of single positive targets. To calculate lysis, target cells were pre-stained with CellTrace Violet to differentiate them from CAR T cells in the downstream flow cytometry analysis (Figure S4). Both FLT3 and CD33 zipFvs can induce high SUPRA CAR T cell cytotoxicity when combined with single FLT3+ K562 and CD33$^+$ K562 in an E:T dependent manner, respectively (Figure 3D). Importantly, at our optimized dosages, we observed significantly higher IFNy secretion from the SUPRA system in on-target conditions when compared to conventional CARs co-cultured at the same E:T ratio (Figures S5A and S5B). This indicates that our dose optimization can also maximize CAR activation compared to constitutively active CAR designs. In addition, to confirm that the FLT3 and CD33 SUPRA CAR system can function as an OR gate against two single positive populations of target cells simultaneously, we pre-stained FLT3+ K562 with Cell Trace Violet and mixed them with the CD33$^+$ K562 targets, which express GFP, in a 1:1 ratio as half the total target cell number with the addition of the both targeting zipFvs, and observed that the zipFvs could successfully trigger SUPRA CAR T cells cytotoxicity against their corresponding target in the mixed target coculture (Figure 3D). This additional condition confirms effective targeting of our system against two cell populations with distinct expression profiles of our target antigens simultaneously, in contrast to one cell population expressing both antigens at uniform levels.

We further tested this system against the cell line MV4-11, an AML cell line derived from the blast cells of a 10-year-old male with biphenotypic B-myelomonocytic leukemia that carries the FLT3-ITD mutation, MOLM-13, an AML cell line derived from the peripheral blood of a 20-year-old male with relapsed AML containing the FLT3-ITD mutation, and THP-1, a human monocytic leukemia cell line. All three cell lines have high CD33 expression and detectable amounts of FLT3 antigen expression, and thus are expected to induce cytotoxicity for FLT3 and CD33 SUPRA systems (Figure 3B). MV4-11, MOLM-13 or THP-1 cells were mixed with FLT3, or CD33 zipFv alone or together, and co-cultured with SUPRA CAR T cells for 24 h under different E:T ratios. As expected, SUPRA CAR T cells showed high target cell killing efficiency when either or both zipFvs were present that

(C) To determine the optimal zipFv dose for each target, RR CAR and target cells were co-cultured at an E:T of 2:1 with varied doses of zipFv, followed by an IFNy ELISA of the supernatant collected 24 h later. A dose of >100 ng of FLT3 zipFv and 25 ng of CD33 zipFv resulted in maximal activation.
(D) Using 125 ng of FLT3 zipFv and 25 ng of CD33 zipFv, cytotoxicity against each single positive K562 target as well as an equal mix of both targets, was determined across a range of E:T ratios to confirm effective killing at these doses.
(E) Cytotoxicity against AML cell lines MV4-11, THP-1, and MOLM-13 was also determined using the same zipFv doses across a range of E:T ratios. Values shown are the means of technical triplicate samples with error bars indicating ±1 standard deviation.

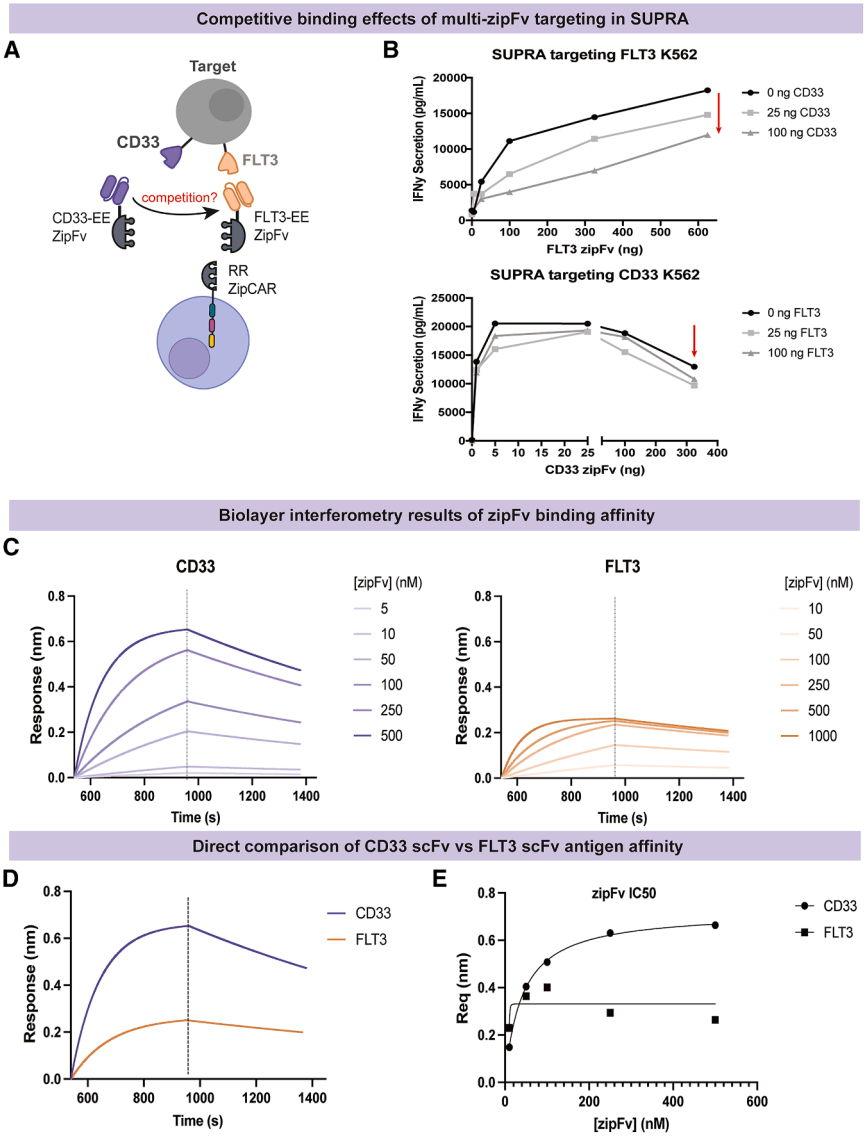

Figure 4. Characterization of competition due to differential affinity of FLT3 and CD33 scFvs to their cognate antigen

(A) Schematic of potential competitive effect between zipFvs when both are present in the system.

(B) A dose competition assay was conducted by measuring IFNy secretion of zipCAR primary T cells when varying amounts of interfering zipFv were added to co-culture with single positive K562 targets. A decrease in activity against the FLT3+ K562 target is observed in the presence of increasing amounts of CD33 zipFv. This is not observed against CD33$^+$ K562 targeting, although a Hook effect is observable at CD33 zipFv amounts over 25 ng.

(C) Biolayer interferometry of zipFv association and dissociation of tips coated in cognate antigen over a range of zipFv concentrations shows differential affinity of each zipFv.

(D) Direct comparison of BLI response at maximum zipFv dose shows a significantly higher association of CD33 zipFv compared to FLT3 zipFv.

(E) Plotting BLI response at equilibrium against the concentration of zipFv was used to calculate the IC50 of each protein, resulting in a CD33 IC_{50} of 41.0 nM and an FLT3 IC_{50} of 247.2 nM.

increased in an E:T dependent manner (Figure 3E), as well as significant IFNy secretion over no zipFv conditions (Figures S5C and S5D). We repeated these experiments across different donor-derived SUPRA CAR-T cells, and observed some donor-to-donor variability, specifically in the basal cytotoxicity without zipFv (Figure S6A). These background levels were similar to basal activity of donor-matched mock transduced CD3$^+$ T cell controls, and similar variability was observed in conventional CD33 and FLT3 CAR activity against the AML cell lines (Figure S6B).

Characterization of differential binding affinity of CD33 and FLT3 zipFvs

Given the observed difference in dose-dependent activity of the FLT3 and CD33 zipFvs, we sought to investigate any potential competition or interference between them when both are present in the SUPRA system that could limit the efficacy against either target (Figure 4A). In this experiment, we created a dose-response matrix against each target as a co-culture of SUPRA CAR primary T cells targeting single positive K562 targets with increasing amounts of "interfering" zipFv added into the system. From this assay, we see significant decreases in IFNy secretion when FLT3 zipFv is used to target FLT3+ K562 in the presence of increasing amounts of CD33 zipFv (Figure 4B). In contrast, the addition of FLT3 zipFv in the system targeting CD33$^+$ K562 with CD33 zipFv does not show the same degree of decreased IFNy production, but we do observe a marked Hook effect at concentrations of CD33 zipFv above 25 ng (Figure 4B). Since the leucine zipper side of the zipFv protein is identical in both designs and previously characterized by our group to not homodimerize,[35] this indicates that this behavior likely results from differences in the affinity of the FLT3 and CD33 scFvs to their cognate antigen in addition to the different expression levels of each antigen on the target cell lines. If the FLT3 antibody fragment has lower affinity to the FLT3 target antigen, the probability of an effective binding event between the FLT3 zipFv and both the target antigen and zipCAR T cell decreases and is likely to be more sensitive to interference from excess, non-targeting CD33 zipFv in the culture. Conversely, if the affinity of the CD33 antibody fragment is high enough to be favored over the affinity of the leucine zipper portion of the zipFv to the zipCAR, this increases the probability of CD33 zipFv saturating the available antigen binding sites on the target cell, while excess free

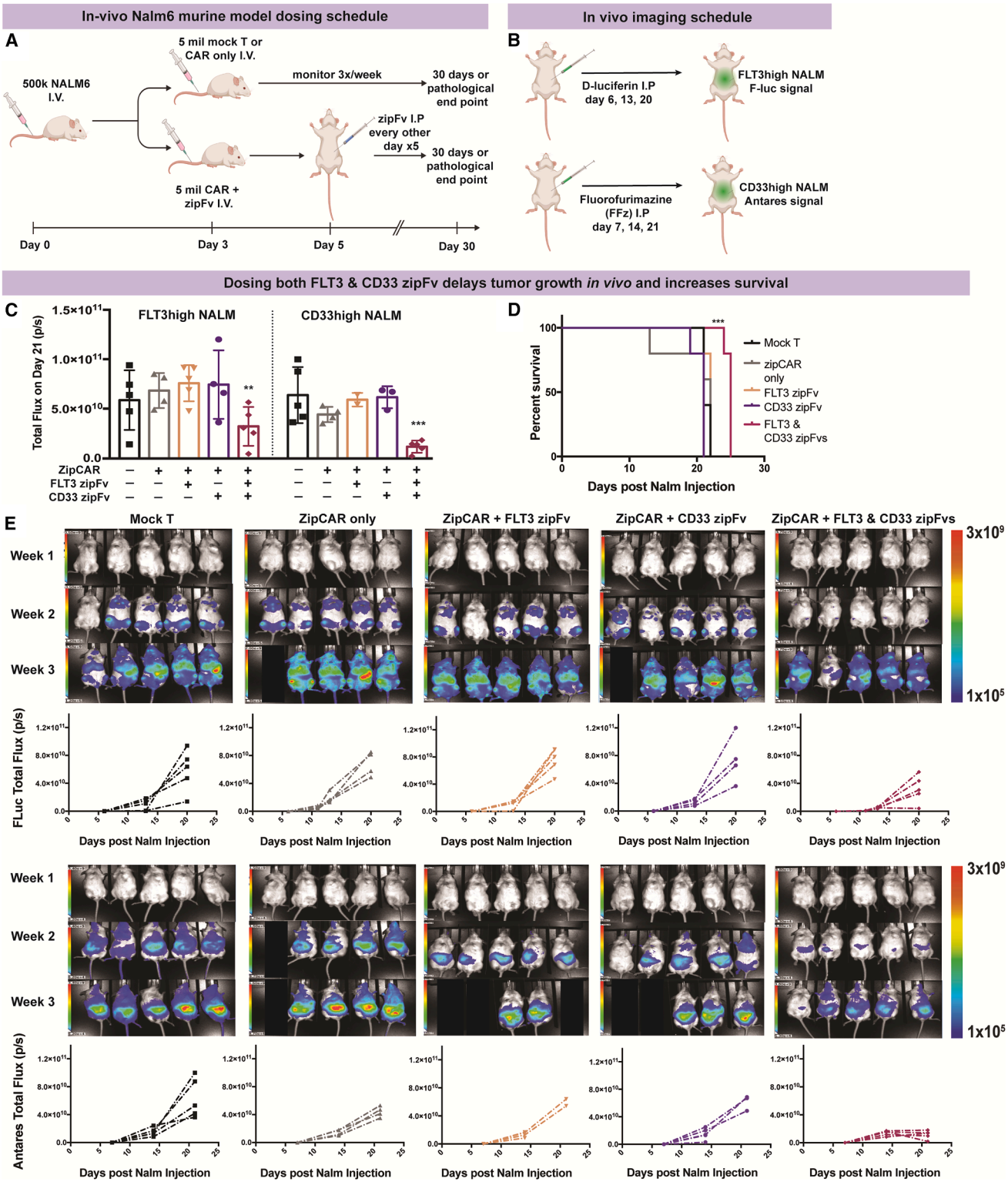

Figure 5. *In vivo* validation of SUPRA OR gate in a xenograft Nalm6 mouse model

(A) Dosing schedule of NOD SCID mice with Nalm6 cells followed by CAR T or mock transduced T cells along with corresponding zipFv.

(B) To independently image FLT3^{high} and CD33^{high} Nalm6 tumor burden, the administration of D-luciferin and FFz were 24 h apart to ensure residual substrate had cleared.

(legend continued on next page)

zipFv in the coculture binds to the zipCAR. In this scenario, the target cell is presenting the cognate leucine zipper half of the bound zipFv, while the CAR-T cell is presenting the scFv portion of the zipFv resulting in an observable Hook effect when the total concentration of zipFv in the co-culture is high enough.

To further characterize potential differences between our zipFvs, we performed bio-layer interferometry (BLI) assays to characterize the affinity of each zipFv to its target FLT3 or CD33 antigen. Biotinylated CD33 and FLT3 proteins were immobilized onto streptavidin tips to characterize the association and dissociation of FLT3-NC7 and CD33-hu195 zipFv at various concentrations (Figure 4C). Based on the results, we clearly see a difference in affinity to their cognate antigen, with CD33 zipFv having a more rapid association (K_a = 1.81 × 10^4 $M^{-1}s^{-1}$) compared to the FLT3 zipFv (K_a = 1.32 × 10^4 $M^{-1}s^{-1}$) (Figure 4D). This difference is also highlighted by plotting BLI response at equilibrium against the concentration of zipFv to determine IC_{50} via non-linear regression, resulting in a CD33 IC_{50} of 41.0 nM and a FLT3 IC_{50} of 247.2 nM (Figure 4E). The molecular weight of the FLT3 zipFv is 40.7 kDa and the molecular weight of the CD33 zipFv is 40.9 kDa. In the context of the maximum quantities used in our interference experiment, 600 ng FLT3 zipFv per 200 μL co-culture is a molar concentration of approximately 74 nM and 300 ng of CD33 zipFv is a molar concentration of 37 nM. Notably, the molar concentrations of CD33 in our interference assay align closely with the IC_{50} value measured by BLI – 100 ng of CD33 zipFv (∼12.5 nM) is within the dynamic range of its IC50 of 41.0 nM, and 300 ng (∼37 nM) approaches saturation. At these concentrations, we observe the emergence of a Hook effect that is subtle at 100 ng and pronounced at 300 ng, consistent with a scenario in which excess CD33 zipFv saturates available antigen on the target cells while unbound zipFv engages the CAR, preventing effective synapse formation.

Taken together, these data indicate that the observed interference and Hook effects in co-culture are consistent with the relative affinities of each zipFv for their target antigens. The higher affinity and lower IC_{50} of the CD33 zipFv allows it to more efficiently engage both the target antige4n and zipCAR even at lower molecular concentrations, contributing to its dominance in mixed-zipFv conditions and its susceptibility to Hook-like inhibition at higher doses. In contrast, the weaker binding of the FLT3 zipFv makes it more vulnerable to competitive displacement or masking effects from excess CD33 zipFv. These results underscore the importance of interrogating the dynamics of multiplexed targeting systems as well as highlight the importance of identifying optimal combinatorial dosing of all adapters in a split CAR system to achieve robust multi-antigen engagement.

In vivo validation of OR gate functionality in a xenograft mouse model

To test the OR gate *in vivo*, we first sought to establish a cancer cell line with a single positive target expression. The Nalm6 B-cell precursor ALL cell line was characterized to have moderate expression of CD33 antigen, and low expression of FLT3, designated as $CD33^{high}$ Nalm6 (Figure S7A). While Nalm6 is not an AML cell line, it is a well-characterized *in vivo* blood cancer model that is relatively easy to engineer to express our target antigens and enables initial *in vivo* validation of our system. To generate a FLT3+ line, Nalm6 cells were transduced to express human FLT3 antigen under antibiotic selection and designated as $FLT3^{high}$ Nalm6 (Figure S7A). We then validated that these cell lines can be effectively killed by our SUPRA system *in vitro* at the previously identified doses of 100 ng FLT3 zipFv and 25 ng CD33 zipFv in 24-h co-culture cytotoxicity experiments at various E:T ratios as previously described (Figure S7B). Lastly, to visualize both cell lines *in vivo* simultaneously, the $FLT3^{high}$ Nalm6 cells were transduced to express Firefly luciferase while the $CD33^{high}$ Nalm6 were transduced to express the orthogonal Antares luciferase (Figure S7C).

We have shown previously that our SUPRA system has *in vivo* activity with zipFv dose ranges between 0.4 mg/kg and 5 mg/kg. Given the extensive dose range characterization we performed *in vitro*, we anticipated that some dose optimization would be needed *in vivo* as well, especially concerning the potential Hook effect with the high-affinity CD33 zipFv. To estimate the effective dose range, we calculated a rough scaling of the *in vitro* dose of 25 ng CD33 zipFv to an *in vivo* dose of 0.3 mg/kg given a total mouse blood volume of 2 mLs (Figure S8). To cover a range across this dose and capture a high dose, we chose 0.15 mg/kg, 0.6 mg/kg, and 3 mg/kg of CD33 zipFv as an initial dosing trial against $CD33^{high}$ Nalm6 with two mice per group following the dosing schedule shown in Figure 5A. Based on this initial trial, the 0.6 mg/kg and 0.15 mg/kg doses proved more effective at reducing tumor burden than the 3 mg/kg group and control groups containing zipCAR only or mock transduced T cells (Figure S9A). For FLT3 zipFv dosing, we chose a higher range of 0.75 mg/kg, 1.5 mg/kg, and 3 mg/kg given its lower affinity than the CD33 zipFv. As expected, our initial dosing trials did not show a marked Hook effect for the FLT3 zipFv targeting $FLT3^{high}$ Nalm6, with the higher doses of 3 mg/kg and 1.5 mg/kg outperforming the lower dose of 0.75 mg/kg in controlling tumor burden (Figure S9B). Given these initial trial results, we chose a dose of 0.6 mg/kg CD33 zipFv and 1.5 mg/kg FLT3 zipFv for our dual target model.

To test the system against eliminating both $CD33^{high}$ and $FLT3^{high}$ Nalm6 cell lines simultaneously, each NOD SCID NSG mouse was injected i.v. with a 1:1 mix of both lines on day

(C) Mice given both FLT3 and CD33 zipFv had significantly decreased tumor burden of both cell lines at week 3 compared to those with no zipFv or either zipFv alone.

(D) Mice given both FLT3 and CD33 zipFv had significantly increased survival rate than those given no zipFv or only FLT3 zipFv.

(E) Monitoring of $FLT3^{high}$ Nalm6 growth via Firefly luciferase luminescence shows that FLT3 only zipFv administration was insufficient to control the tumor burden, while the group given both zipFvs had a significant reduction in tumor burden across the monitoring period leading to a substantial delay in tumor growth. Monitoring of $CD33^{high}$ Nalm6 growth via Antares luciferase luminescence also shows that only the group given both CD33 and FLT3 zipFvs has a significant decrease in tumor growth rate across the treatment and sustained reduction in $CD33^{high}$ Nalm6 cells. Statistical analysis using unpaired two-tailed *t* test was performed. Not significant $p > 0.05$, $^{*}p < 0.05$, $^{**}p < 0.01$, $^{***}p < 0.001$.

0 (250k each) followed by T cell injection of either zipCAR only, zipCAR incubated with the first dose of zipFv, or mock transduced $CD3^+$ T cells on day 3. Of the three groups that received the full SUPRA system, one group only received FLT3 zipFv, one group received only CD33 zipFv, while the complete OR gate group received both CD33 and FLT3 zipFvs and showed increased survival compared to the remaining groups (Figure 5D). Growth of the $FLT3^{high}$ Nalm6-Firefly luciferase cells was monitored via IVIS imaging of the luciferase signal following i.p injection of D-Luciferin (Figure 5B), and while the FLT3 zipFv only group showed some delay in tumor growth as seen in the week 2 luminescence images, only the group given both zipFvs showed a significant reduction in $FLT3^{high}$ tumor burden over the entire treatment period (Figures 5C and 5E). Growth of the $CD33^{high}$ Nalm6-Antares luciferase cells was similarly monitored via IVIS imaging following the i.p injection of fluorofurimazine. Similarly, only the group given both FLT3 and CD33 zipFvs showed an effective reduction in tumor growth rate that persisted after the last dose was administered (Figures 5C and 5E). These studies indicate preliminary *in vivo* efficacy of dosing both zipFvs as an OR gate in a mixed target model and serve to highlight the importance of dose optimization in the development of effective therapies.

We then sought to further test the activity of the system *in vivo* against an AML model. To that end, we engineered the MOLM-13 cell line to express Firefly luciferase under antibiotic selection to ensure stable expression. To evaluate the growth kinetics of this tumor model *in vivo*, we injected NOD SCID mice with 250k MOLM-13 cells and observed aggressive tumor progression resulting in physiological endpoint between 16 and 18 days post injection. Importantly, a control condition with both MOLM-13 cells and zipFV dosed every other day without CAR T-cells showed no impact on tumor burden, indicating the zipFv lacks *in vivo* activity on its own (Figure 6C). Based on these growth kinetics, we chose to inject both MOLM-13 and either zipCAR-T cells incubated with the first dose of both zipFvs, or conventional CD33 CAR T cells on day 0 followed by zipFv dosing every other day for a total of eight doses (Figure 6A). Tumor burden was imaged via D-Luciferin injection each week until day 21 or physiological endpoint (Figure 6B). Despite the limited group size, the mice that received the complete OR Gate had minimal inter-mouse variability, and the magnitude of differences in tumor burden resulted in an unpaired *t* test *p* value of <0.001, emphasizing the consistency of the observed control of tumor burden compared to zipCAR only (Figure 6D). While the conventional CD33 CAR initially slowed tumor growth, tumor burden gradually increased over time to approach control levels by day 16. In contrast, the zipFv system maintained durable control over the tumor, resulting in substantially lower overall tumor burden (Figure 6D). This small-scale trial further supports the therapeutic potential of targeting both FLT3 and CD33 as a more effective method of eliminating AML tumor cells compared to a single target conventional CAR.

HSPC sparing and identification of a potentially effective dose range

As a preliminary indication of the safety profile of our SUPRA system, we sought to identify a therapeutic window of activity *in vitro* that spares primary human hematopoietic stem and progenitor cells (HSPCs) from ablation while retaining cytotoxic activity against cancer cell lines. We obtained bone marrow or cord blood derived $CD34^+$ enriched human HSPCs (StemCell) and characterized their expression of the target antigens CD33 and FLT3 using the same antibody binding capacity assay previously described (Figure 7A). The bulk $CD34^+$ population of both stem and progenitor cells showed moderate CD33 expression and low FLT3 expression (Figure 7B). CD90 has been identified as a marker that differentiates HSCs from multipotent, erythro-myeloid, and lympho-myeloid progenitors.[48] By gating for the $CD34^+CD90^+$ subset, we quantified the expression of CD33 and FLT3 within this population and found it to be slightly enriched in FLT3 and lower in CD33 expression (Figures 7A and 7C). Given the limited number of this HSC-enriched population, we chose one E:T ratio of 2:1 to test the dose-dependent cytotoxic activity of the SUPRA system against these cells in a 24-h co-culture. To assess cytotoxicity, HSPCs were isolated from T cells as $CD3^-CD34^+$ followed by further gating of a $CD90^+$CD45RA- HSC-enriched subset (Figure 7D). Compared to the cytotoxic activity against our *in vivo* model Nalm6 cell lines, we observed minimal toxicity when targeting FLT3 that was slightly higher in the HSC-enriched subset, and a maximum of ~30% toxicity when targeting CD33 at our highest dosage (Figure 7E). Given our utilized therapeutic dosages of 100–125 ng of FLT3 zipFv and 25 ng of CD33 zipFv, there is minimal toxicity against the HSPCs at these doses, indicating the existence of a therapeutic dose window for effective specific lysis of cancer cells with minimal off-tumor activity.

DISCUSSION

CAR T cell therapies have proven to be a remarkable breakthrough and exciting area of progress in immunotherapy with long-term proven efficacy.[49] Currently implemented CAR designs suffer from fixed antigen targeting capabilities, allowing for antigen escape, as well as high levels of on-target, off-tumor toxicity due to their non-tunability.[50–55] To overcome these limitations, we have previously introduced our SUPRA CAR platform as a tunable, multiplexed targeting platform. In this study, we adapted SUPRA toward treating AML, a heterogeneous disease with a very poor prognosis that has proven difficult to address with conventional CAR T designs. Among the many antigen markers that have been characterized for AML, we focused on CD33, a myeloid marker shown to be expressed on over 85% of AML cases, and FLT3, a common mutation in AML that has been tied to poor disease progression. We show that we can dose two zipFv adapters simultaneously to achieve combinatorial SUPRA targeting that eliminates target AML cell lines with varying expression levels of CD33 and FLT3. Additionally, we characterized the potential competition present in this system to identify concentrations of each adapter that limit inhibition and account for the variable affinity of each scFv to their target antigen. Interestingly, this translated to *in vivo* dose optimization of FLT3 and CD33 zipFvs, further emphasizing the importance of adapter characterization in split systems. Within our working dose range, we confirmed minimal toxicity against bone marrow or cord blood derived $CD34^+$ HSPCs as well as the smaller

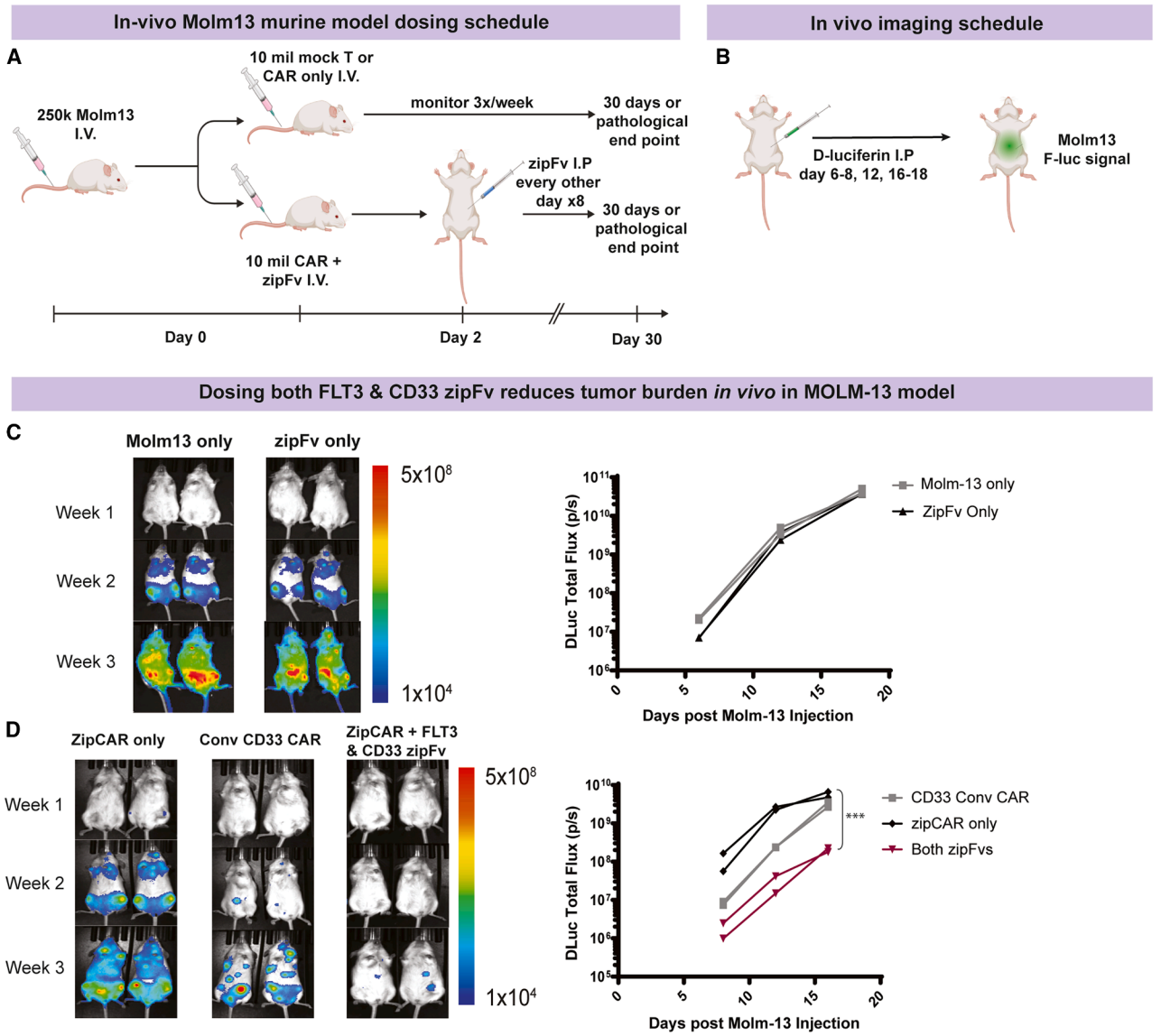

Figure 6. *In vivo* validation of SUPRA OR Gate in a xenograft MOLM-13 mouse model

(A) Dosing schedule of NOD SCID mice injected with MOLM-13 cells engineered to express Firefly luciferase along with CAR-T and corresponding zipFv with additional zipFv dosing every other day for a total of eight doses.

(B) D-luciferin was injected intraperitoneally to visualize tumor burden 3x during experiment duration.

(C) Mice injected with MOLM-13 cells only or MOLM-13 cells along with zipFv only without corresponding zipCAR showed aggressive progression of tumor burden.

(D) Mice injected with zipCAR plus both CD33 and FLT3 zipFvs showed significant (***$p < 0.001$) control of tumor burden compared to those injected with zipCAR only. Conventional CD33 CAR mice showed some initial control of tumor burden that then progressed by week 3

$CD90^{+}CD45RA$- HSC-enriched subset, demonstrating the potential of SUPRA as a treatment strategy that overcomes the high toxicity of conventional CAR treatment.

In our *in vitro* screening experiments, we consistently saw lower basal activation of the zipCAR compared to conventional CAR designs—a direct consequence of the SUPRA system's split configuration, which keeps the CAR in an off state until the zipFv adapter is introduced. This built-in control mechanism enhances safety by uncoupling CAR T cell activation from mere presence in circulation. While this architecture might raise questions about therapeutic potency, our data demonstrate that the SUPRA system can, in fact, elicit stronger functional responses than conventional CARs at optimized doses. Specifically, we observed higher levels of cytokine secretion at optimized zipFv doses, as well as improved tumor control *in vivo* using our MOLM-13 xenograft model. Moreover, the modularity of the SUPRA system allows for fine-tuning of the therapeutic response by adjusting zipFv dosing, enabling scalable activation that can

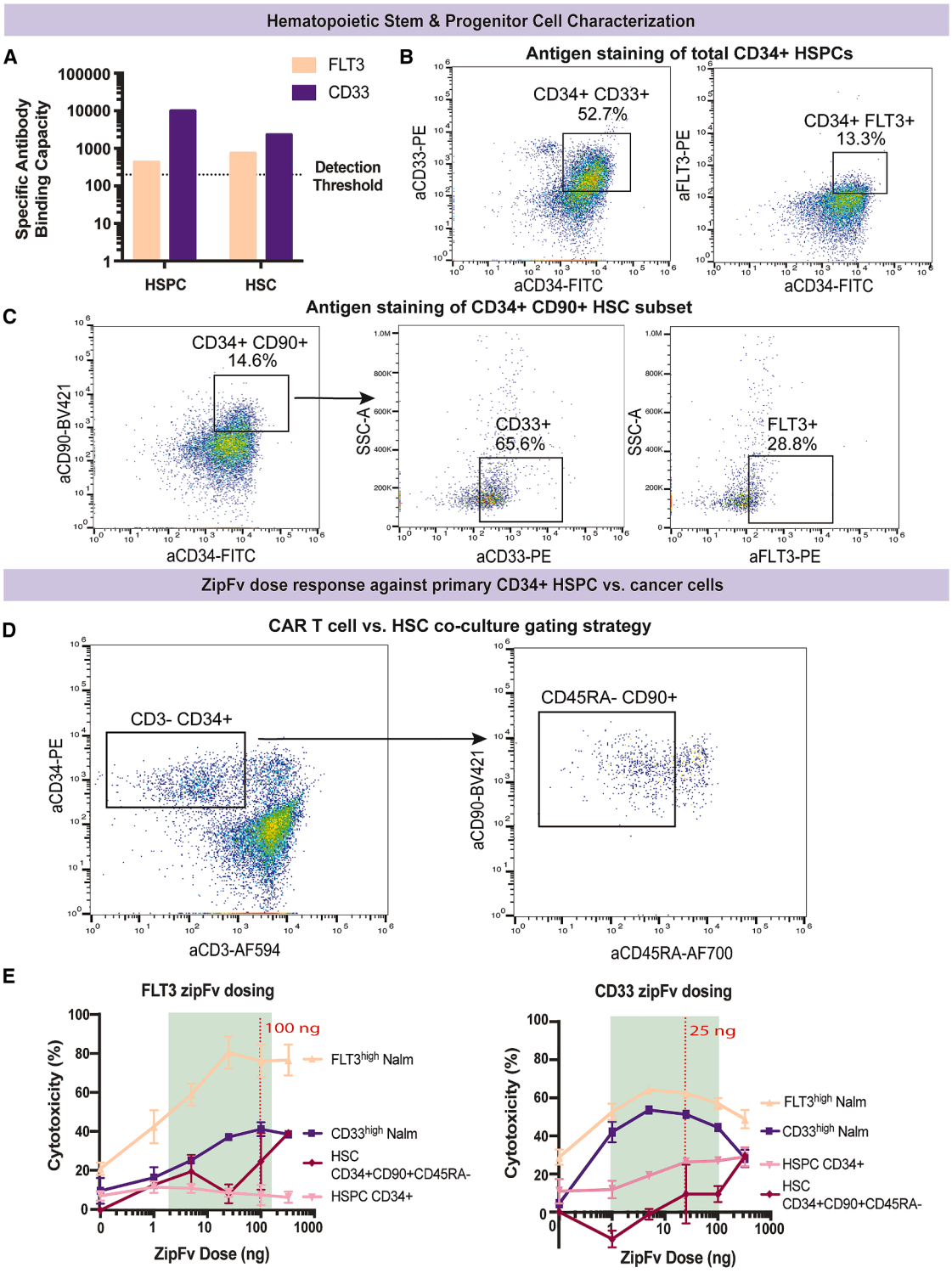

Figure 7. Identification of a therapeutic zipFv dose window that spares healthy HSPCs *in vitro*

(A) CD34 enriched HSPCs were obtained as cryopreserved vials from StemCell and stained for antigen expression. MESF quantification of total CD34$^+$ HSPC expression of the target antigens shows a moderate expression of CD33 and low expression of FLT3 while the CD90$^+$ stem-like subset had lower CD33 and higher FLT3 expression.

(B) HSPCs were gated for CD34 expression along with either antigen of interest.

(C) The subpopulation of CD90$^+$ cells makes up 10%–15% of the total HSPC population with varying levels of antigen expression.

(legend continued on next page)

be tailored for maximal efficacy or minimized for safety depending on the clinical context. In early 2020, AbbVie and Calibr initiated the first clinical trial of a "switchable" anti-CD19 CAR design composed of an antibody switch as the adapter to the CAR, motivated by the need to develop safer and more controllable CAR designs.[56] Initial results shared in late 2022 showed that 6 out of 9 patients with relapsed/refractory B cell malignancies treated with CLBR001+SWI019 had a complete response with only one dose CAR-T (CLBR001) and cognate antibody switch (SWI019).[57] Additionally, these patients experienced lower levels of CRS toxicity, if at all. Like SUPRA, the CLBR001+SWI019 system relies on a biologically derived fusion protein adapter, therefore these preliminary results are an exciting demonstration of the potential of such split CAR designs to combat conventional CAR T treatment toxicity while retaining therapeutic efficacy.

In this study, we focused on just two target antigens, CD33 and FLT3, to demonstrate the feasibility of a SUPRA OR gate against AML. FLT3, and CD33 are well-established AML-associated antigens with distinct but overlapping expression patterns across disease stages. CD33 is broadly expressed in over 80% of AML cases and tends to be retained even at relapse, although its surface density can vary between patients and disease subtypes. FLT3, in contrast, is mutated in approximately 25% of AML patients, and these clones frequently expand at relapse, contributing to poor prognosis. Notably, FLT3-ITD+ AML has been correlated with elevated CD33 expression, making dual targeting of these antigens a rational strategy to address both disease heterogeneity and clonal evolution. Current targeted therapies such as gilteritinib (FLT3 inhibitor) and gemtuzumab ozogamicin (anti-CD33 ADC) are approved for subsets of patients but are limited by issues such as resistance, off-tumor toxicity, and transient responses.[58,59] In contrast, our SUPRA OR-gate design enables combinatorial targeting of both FLT3 and CD33 with a single, modular CAR T platform. This approach offers enhanced potency while preserving safety, and, most importantly, introduces a level of dosing flexibility not possible with conventional CARs. Additionally, the flexibility of the SUPRA system offers the potential to switch or add additional antigen targets depending on the individual patient's disease phenotype, making SUPRA particularly well suited for managing relapsed/refractory AML where antigen profiles are dynamic. We have also demonstrated both "AND" and "NOT" logic in SUPRA previously, which can be coupled with this OR gate design to further increase the specificity of the circuit against cancer target cells. Given the characterization we have done here, it will be important to explore the interaction between adapter binding affinity and the relative abundance of each target to design effective combinatorial targeting strategies as we increase the complexity of these systems.

This study demonstrates proof-of-concept efficacy of our SUPRA platform for combinatorial targeting against complex disease indications, and there are several directions that could be explored to further strengthen the SUPRA platform and advance its clinical readiness. For example, while our library of orthogonal leucine zippers spans a range of affinities that can be leveraged to tune response strength, further optimization of affinity and pharmacokinetic properties can be explored to balance the scFv antigen binding affinities and increase the adapter half-life. Advances in computational protein design and AI-assisted optimization can provide new avenues to revisit historical design constraints, such as the extracellular spacing of the leucine zipper domains, or identify novel positions for protein modifications (PEGylation or glycoengineering) that increase the half-life of the scFv and reduce the requirement for repeat dosing. Ongoing studies in murine models are currently evaluating zipFv pharmacokinetics to better define exposure profiles and optimal dosing schedules for future translation into clinical models. Finally, an additional advantage of the SUPRA platform is its enhanced safety profile given emerging strategies for *in vivo* induction of CAR T cells. Recent clinical trials assessing the feasibility of *in vivo* generation of CAR T have had serious safety concerns, with the majority of patients experiencing grade 3 or higher SAEs.[60] In principle, SUPRA could mitigate these toxicities as the zipCAR-expressing cells generated *in vivo* would remain inert until zipFv administration. Furthermore, zipFv could be dosed on an incremental schedule to add an additional layer of control against severe CRS. Future studies evaluating this approach in clinically relevant *in vivo* CAR delivery systems and toxicity models will be important for determining the translational feasibility and readiness for early phase clinical evaluation.

Limitations of the study

It is necessary to acknowledge several limitations of this study. First, the cytotoxicity experiments were conducted using established or engineered cell lines as targets rather than primary patient AML samples, which can exhibit greater heterogeneity in antigen expression and clonal composition that may influence efficacy in a clinical setting. Second, while the *in vitro* HSPC sparing assay provides a useful preliminary safety assessment, it does not account for the complexity of *in vivo* hematopoiesis, including trafficking of stem and progenitor cells between the bone marrow and periphery, differences in maturation states, and the potential cumulative effects of repeated zipFv dosing on long-term hematopoietic reconstitution. Finally, while the MOLM-13 xenograft model provided encouraging proof-of-concept *in vivo* data, it involved a limited number of animals per group. Larger, adequately powered studies will be necessary

(D) In co-culture conditions with the SUPRA system, HSPCs were first gated as $CD3^{-}$, $CD34^{+}$ followed by further subclassification of an HSC-enriched subset as CD45RA- $CD90^{+}$ within the HSPC population.

(E) Primary $CD3^{+}$ T cells expressing RR zipCAR were co-cultured with healthy HSPCs at an E:T of 2:1 for 24 h in the presence of a range of zipFv doses. In the HSPC $CD34^{+}$ condition, 15,000 target cells and 30,000 CAR T cell were plated, and an average of 16,321 viable target cells were recovered post co-culture in the target only condition. In the HSC targeted condition, 10,000 target cells and 20,000 CAR T cells were plated, and an average of 7,594 viable target cells were recovered post coculture in the target only condition. By comparing to the cytotoxic activity against our Nalm6 target cells, we can identify a therapeutic window of >50% activity against the target cells that has <30% toxicity against the HSPCs for both zipFvs. Data are plotted as the mean of three technical replicates with error bars indicating ±1 standard deviation.

to fully characterize the therapeutic efficacy and durability of the SUPRA OR gate in AML.

RESOURCE AVAILABILITY

Lead contact

Further information and requests for resources and reagents should be directed to and will be fulfilled by the lead contact, Wilson W. Wong (wilwong@bu.edu).

Materials availability

All plasmid constructs and cell lines generated in this study will be made available on request, but we may require a payment and/or a completed materials transfer agreement if there is potential for commercial application.

Data and code availability

- All data reported in this study will be shared by the lead contact upon request.
- This study does not report original code.
- Any additional information required to reanalyze the data reported in this study is available from the lead contact upon request.

ACKNOWLEDGMENTS

W.W.W. acknowledges funding from NIH Award (U01CA265713). M.Y.S. acknowledges funding from NIH F31 Award (1F31HL162477-01A1). We also thank Wong lab members for suggestions on the manuscript; Grinstaff lab members for assistance on the BLI assay; BU IVIS imaging core facility for mice *in vivo* imaging (NIH grant 1S10RR024523-01).

AUTHOR CONTRIBUTIONS

M.Y.S. designed and performed primary T cell, HSPC experiments and *in vivo* studies, analyzed the data, and generated figures. J.C. designed and performed Jurkat screening experiments and assisted M.Y.S. with primary T cell experiments and *in vivo* studies. J.Z.H. assisted with the production and purification of zipFv and with MOLM-13 *in vivo* studies. M.L. performed BLI assays and generated corresponding figures. S.L. assisted with *in vitro* zipFv functional screening. H.D., Y.L., N.L., and T.L designed and generated CD33 and FLT3 binders and zipFv constructs, engineered K562 target cell lines, and advised on *in vivo* and HSPC experiments with input and supervision from N.F., B.S.G., and M.G.A. W.W.W. conceived and supervised the project and analyzed the data. All authors commented on and approved the study.

DECLARATION OF INTERESTS

W.W.W. is a scientific co-founder and shareholder of Senti Biosciences and 4Immune.

STAR★METHODS

Detailed methods are provided in the online version of this paper and include the following:

- KEY RESOURCES TABLE
- EXPERIMENTAL MODEL AND STUDY PARTICIPANT DETAILS
  - Source of primary human T cells
  - Animals
- METHOD DETAILS
  - Cell line culture
  - zipFv and zipCAR construct design
  - Expression and purification of zipFv
  - Western blot and SDS-PAGE gel electrophoresis
  - Primary human T cell isolation and culture
  - Lentivirus generation and transduction of human T cells
  - *In-vitro* NFAT Jurkat activation assay
  - Antibody binding capacity assay
  - *In-vitro* cytotoxicity assays
  - Cytokine release assay
  - zipFv competition assay
  - Biolayer interferometry assay
  - HSPC sparing assay
  - Xenograft mouse models
  - Statistical analysis

SUPPLEMENTAL INFORMATION

Supplemental information can be found online at https://doi.org/10.1016/j.isci.2026.117008.

Received: February 9, 2026
Revised: March 27, 2026
Accepted: May 28, 2026

REFERENCES

1. Döhner, H., Weisdorf, D.J., and Bloomfield, C.D. (2015). Acute Myeloid Leukemia. New England J. Med. *373*, 1136–1152. https://doi.org/10.1056/NEJMra1406184.
2. Acute Myeloid Leukemia — Cancer Stat Facts. https://seer.cancer.gov/statfacts/html/amyl.html.
3. Long, L., Assaraf, Y.G., Lei, Z.N., Peng, H., Yang, L., Chen, Z.S., and Ren, S. (2020). Genetic biomarkers of drug resistance: A compass of prognosis and targeted therapy in acute myeloid leukemia. Drug Resist. Updat. *52*, 100703. https://doi.org/10.1016/j.drup.2020.100703.
4. Bazarbachi, A., Bug, G., Baron, F., Brissot, E., Ciceri, F., Dalle, I.A., Döhner, H., Esteve, J., Floisand, Y., Giebel, S., et al. (2020). Clinical practice recommendation on hematopoietic stem cell transplantation for acute myeloid leukemia patients with FLT3-internal tandem duplication: a position statement from the Acute Leukemia Working Party of the European Society for Blood and Marrow Transplantation. Haematologica *105*, 1507–1516. https://doi.org/10.3324/haematol.2019.243410.
5. Cornelissen, J.J., and Blaise, D. (2016). Hematopoietic stem cell transplantation for patients with AML in first complete remission. Blood *127*, 62–70. https://doi.org/10.1182/blood-2015-07-604546.
6. Takami, A. (2018). Hematopoietic stem cell transplantation for acute myeloid leukemia. Int. J. Hematol. *107*, 513–518. https://doi.org/10.1007/s12185-018-2412-8.
7. Short, N.J., Konopleva, M., Kadia, T.M., Borthakur, G., Ravandi, F., DiNardo, C.D., and Daver, N. (2020). Advances in the treatment of acute myeloid leukemia: New drugs and new challenges. Cancer Discov. *10*, 506–525. https://doi.org/10.1158/2159-8290.cd-19-1011.
8. Capria, S., Trisolini, S.M., Diverio, D., Minotti, C., Breccia, M., Cartoni, C., Carmini, D., Gozzer, M., La Rocca, U., Shafii Bafti, M., and Martelli, M. (2022). Autologous stem cell transplantation in favorable-risk acute myeloid leukemia: single-center experience and current challenges. Int. J. Hematol. *116*, 586–593. https://doi.org/10.1007/s12185-022-03370-4.
9. Awada, H., Mustafa Ali, M.K., Thapa, B., Awada, H., Seymour, L., Liu, L., Gurnari, C., Kishtagari, A., Wang, E., and Baer, M.R. (2022). A Focus on Intermediate-Risk Acute Myeloid Leukemia: Sub-Classification Updates and Therapeutic Challenges. Cancers *14*, 4166. https://doi.org/10.3390/cancers14174166.
10. Stelmach, P., and Trumpp, A. (2023). Leukemic stem cells and therapy resistance in acute myeloid leukemia. Haematologica *108*, 353–366. https://doi.org/10.3324/haematol.2022.280800.
11. King, C., PharmD, B.C.O.P.,A., Orozco, S., and PharmD, J. (2019). Axicabtagene Ciloleucel: The First FDA-Approved CAR T-Cell Therapy for Relapsed/Refractory Large B-Cell Lymphoma. J. Adv. Pract. Oncol. *10*, 878.

12. Maude, S.L., Laetsch, T.W., Buechner, J., Rives, S., Boyer, M., Bittencourt, H., Bader, P., Verneris, M.R., Stefanski, H.E., Myers, G.D., et al. (2018). Tisagenlecleucel in Children and Young Adults with B-Cell Lymphoblastic Leukemia. N. Engl. J. Med. *378*, 439–448. https://doi.org/10.1056/nejmoa1709866.

13. Abramson, J.S., Palomba, M.L., Gordon, L.I., Lunning, M.A., Wang, M., Arnason, J., Mehta, A., Purev, E., Maloney, D.G., Andreadis, C., et al. (2020). Lisocabtagene maraleucel for patients with relapsed or refractory large B-cell lymphomas (TRANSCEND NHL 001): a multicentre seamless design study. Lancet *396*, 839–852. https://doi.org/10.1016/s0140-6736(20)31366-0.

14. Munshi, N.C., Anderson, L.D., Jr., Shah, N., Madduri, D., Berdeja, J., Lonial, S., Raje, N., Lin, Y., Siegel, D., Oriol, A., et al. (2021). Idecabtagene Vicleucel in Relapsed and Refractory Multiple Myeloma. N. Engl. J. Med. Overseas. Ed. *384*, 705–716. https://doi.org/10.1056/nejmoa2024850.

15. Wang, Y., Jain, P., Locke, F.L., Munoz, J., Maurer, M.J., Beitinjaneh, A., Frank, M.J., Dahiya, S., McGuirk, J.P., Jacobs, M.T., et al. (2021). Brexucabtagene Autoleucel for Relapsed/Refractory Mantle Cell Lymphoma: Real World Experience from the US Lymphoma CAR T Consortium. Blood *138*, 744. https://doi.org/10.1182/blood-2021-147563.

16. Berdeja, J.G., Madduri, D., Usmani, S.Z., Jakubowiak, A., Agha, M., Cohen, A.D., Stewart, A.K., Hari, P., Htut, M., Lesokhin, A., et al. (2021). Ciltacabtagene autoleucel, a B-cell maturation antigen-directed chimeric antigen receptor T-cell therapy in patients with relapsed or refractory multiple myeloma (CARTITUDE-1): a phase 1b/2 open-label study. Lancet *398*, 314–324. https://doi.org/10.1016/S0140-6736(21)00933-8.

17. Zhao, J., Song, Y., and Liu, D. (2019). Clinical trials of dual-target CAR T cells, donor-derived CAR T cells, and universal CAR T cells for acute lymphoid leukemia. J. Hematol. Oncol. *12*, 17. https://doi.org/10.1186/s13045-019-0705-x.

18. Mardiana, S., and Gill, S. (2020). CAR T Cells for Acute Myeloid Leukemia: State of the Art and Future Directions. Front. Oncol. *10*, 697. https://doi.org/10.3389/fonc.2020.00697.

19. Zeng, A.G.X., Bansal, S., Jin, L., Mitchell, A., Chen, W.C., Abbas, H.A., Chan-Seng-Yue, M., Voisin, V., van Galen, P., Tierens, A., et al. (2022). A cellular hierarchy framework for understanding heterogeneity and predicting drug response in acute myeloid leukemia. Nat. Med. *28*, 1212–1223. https://doi.org/10.1038/s41591-022-01819-x.

20. Romer-Seibert, J.S., and Meyer, S.E. (2021). Genetic Heterogeneity and Clonal Evolution in Acute Myeloid Leukemia. Curr. Opin. Hematol. *28*, 64–70. https://doi.org/10.1097/moh.0000000000000626.

21. Horibata, S., Gui, G., Lack, J., DeStefano, C.B., Gottesman, M.M., and Hourigan, C.S. (2019). Heterogeneity in refractory acute myeloid leukemia. Proc. Natl. Acad. Sci. USA *116*, 10494–10503. https://doi.org/10.1073/pnas.1902375116.

22. Schorr, C., and Perna, F. (2022). Targets for chimeric antigen receptor T-cell therapy of acute myeloid leukemia. Front. Immunol. *13*, 1085978. https://doi.org/10.3389/fimmu.2022.1085978.

23. Wang, Q.S., Wang, Y., Lv, H.y., Han, Q.w., Fan, H., Guo, B., Wang, L.l., and Han, W.d. (2015). Treatment of CD33-directed chimeric antigen receptor-modified T cells in one patient with relapsed and refractory acute myeloid leukemia. Mol. Ther. *23*, 184–191. https://doi.org/10.1038/mt.2014.164.

24. Cho, J.H., Okuma, A., Sofjan, K., Lee, S., Collins, J.J., and Wong, W.W. (2021). Engineering advanced logic and distributed computing in human CAR immune cells. Nat. Commun. *12*, 792. https://doi.org/10.1038/s41467-021-21078-7.

25. Moghimi, B., Muthugounder, S., Jambon, S., Tibbetts, R., Hung, L., Bassiri, H., Hogarty, M.D., Barrett, D.M., Shimada, H., and Asgharzadeh, S. (2021). Preclinical assessment of the efficacy and specificity of GD2-B7H3 SynNotch CAR-T in metastatic neuroblastoma. Nat. Commun. *12*, 511–515. https://doi.org/10.1038/s41467-020-20785-x.

26. Fedorov, V.D., Themeli, M., and Sadelain, M. (2013). PD-1– and CTLA-4–Based Inhibitory Chimeric Antigen Receptors (iCARs) Divert Off-Target Immunotherapy Responses. Sci. Transl. Med. *5*, 215ra172. https://doi.org/10.1126/scitranslmed.3006597.

27. Zah, E., Nam, E., Bhuvan, V., Tran, U., Ji, B.Y., Gosliner, S.B., Wang, X., Brown, C.E., and Chen, Y.Y. (2020). Systematically optimized BCMA/CS1 bispecific CAR-T cells robustly control heterogeneous multiple myeloma. Nat. Commun. *11*, 2283. https://doi.org/10.1038/s41467-020-16160-5.

28. Srivastava, S., Salter, A.I., Liggitt, D., Yechan-Gunja, S., Sarvothama, M., Cooper, K., Smythe, K.S., Dudakov, J.A., Pierce, R.H., Rader, C., and Riddell, S.R. (2019). Logic-Gated ROR1 Chimeric Antigen Receptor Expression Rescues T Cell-Mediated Toxicity to Normal Tissues and Enables Selective Tumor Targeting. Cancer Cell *35*, 489–503.e8. https://doi.org/10.1016/j.ccell.2019.02.003.

29. Roybal, K.T., Rupp, L., Morsut, L., Walker, W., McNally, K., Park, J., and Lim, W. (2016). Precision Tumor Recognition by T Cells With Combinatorial Antigen-Sensing Circuits. Cell *164*, 770–779. https://doi.org/10.1016/j.cell.2016.01.011.

30. Salzer, B., Schueller, C.M., Zajc, C.U., Peters, T., Schoeber, M.A., Kovacic, B., Buri, M.C., Lobner, E., Dushek, O., Huppa, J.B., et al. (2020). Engineering AvidCARs for combinatorial antigen recognition and reversible control of CAR function. Nat. Commun. *11*, 4166. https://doi.org/10.1038/s41467-020-17970-3.

31. Lanitis, E., Coukos, G., and Irving, M. (2020). All systems go: converging synthetic biology and combinatorial treatment for CAR-T cell therapy. Curr. Opin. Biotechnol. *65*, 75–87. https://doi.org/10.1016/j.copbio.2020.01.009.

32. Savanur, M.A., Weinstein-Marom, H., and Gross, G. (2021). Implementing Logic Gates for Safer Immunotherapy of Cancer. Front. Immunol. *12*, 780399. https://doi.org/10.3389/fimmu.2021.780399.

33. Haubner, S., Mansilla-Soto, J., Nataraj, S., Kogel, F., Chang, Q., de Stanchina, E., Lopez, M., Ng, M.R., Fraser, K., Subklewe, M., et al. (2023). Cooperative CAR targeting to selectively eliminate AML and minimize escape. Cancer Cell *41*, 1871–1891.e6. https://doi.org/10.1016/J.CCELL.2023.09.010.

34. Wermke, M., Kraus, S., Ehninger, A., Bargou, R.C., Goebeler, M.E., Middeke, J.M., Kreissig, C., von Bonin, M., Koedam, J., Pehl, M., et al. (2021). Proof of concept for a rapidly switchable universal CAR-T platform with UniCAR-T-CD123 in relapsed/refractory AML. Blood *137*, 3145–3148. https://doi.org/10.1182/blood.2020009759.

35. Cho, J.H., Collins, J.J., and Wong, W.W. (2018). Universal Chimeric Antigen Receptors for Multiplexed and Logical Control of T Cell Responses. Cell *173*, 1426–1438.e11. https://doi.org/10.1016/j.cell.2018.03.038.

36. Niswander, L.M., Graff, Z.T., Chien, C.D., Chukinas, J.A., Meadows, C.A., Leach, L.C., Loftus, J.P., Kohler, M.E., Tasian, S.K., and Fry, T.J. (2023). Potent preclinical activity of FLT3-directed chimeric antigen receptor T-cell immunotherapy against *FLT3*- mutant acute myeloid leukemia and *KMT2A*-rearranged acute lymphoblastic leukemia. Haematologica *108*, 457–471. https://doi.org/10.3324/haematol.2022.281456.

37. Wang, Y., Xu, Y., Li, S., Liu, J., Xing, Y., Xing, H., Tian, Z., Tang, K., Rao, Q., Wang, M., and Wang, J. (2018). Targeting FLT3 in acute myeloid leukemia using ligand-based chimeric antigen receptor-engineered T cells. J. Hematol. Oncol. *11*, 60. https://doi.org/10.1186/s13045-018-0603-7.

38. Godwin, C.D., Gale, R.P., and Walter, R.B. (2017). Gemtuzumab ozogamicin in acute myeloid leukemia. Leukemia *31*, 1855–1868. https://doi.org/10.1038/leu.2017.187.

39. Molica, M., Perrone, S., Mazzone, C., Niscola, P., Cesini, L., Abruzzese, E., and de Fabritiis, P. (2021). CD33 Expression and Gentuzumab Ozogamicin in Acute Myeloid Leukemia: Two Sides of the Same Coin. Cancers (Basel) *13*, 3214. https://doi.org/10.3390/cancers13133214.

40. Cortes, J.E., de Lima, M., Dombret, H., Estey, E.H., Giralt, S.A., Montesinos, P., Röllig, C., Venditti, A., and Wang, E.S. (2020). Prevention, recognition, and management of adverse events associated with gemtuzumab ozogamicin use in acute myeloid leukemia. J. Hematol. Oncol. *13*, 137–138. https://doi.org/10.1186/s13045-020-00975-2.

41. Subklewe, M., Stein, A., Walter, R.B., Bhatia, R., Wei, A.H., Ritchie, D., Bücklein, V., Vachhani, P., Dai, T., Hindoyan, A., et al. (2019). Preliminary

Results from a Phase 1 First-in-Human Study of AMG 673, a Novel Half-Life Extended (HLE) Anti-CD33/CD3 BiTE® (Bispecific T-Cell Engager) in Patients with Relapsed/Refractory (R/R) Acute Myeloid Leukemia (AML). Blood *134*, 833. https://doi.org/10.1182/blood-2019-127977.

42. Marcinek, A., Brauchle, B., Rohrbacher, L., Hänel, G., Philipp, N., Märkl, F., Strzalkowski, T., Lacher, S.M., Udiljak, D., Spiekermann, K., et al. (2023). CD33 BiTE® molecule-mediated immune synapse formation and subsequent T-cell activation is determined by the expression profile of activating and inhibitory checkpoint molecules on AML cells. Cancer Immunol. Immunother. *72*, 2499–2512. https://doi.org/10.1007/S00262-023-03439-X/FIGURES/6.

43. Daver, N., Schlenk, R.F., Russell, N.H., and Levis, M.J. (2019). Targeting FLT3 mutations in AML: review of current knowledge and evidence. Leukemia *33*, 299–312. https://doi.org/10.1038/s41375-018-0357-9.

44. Giannakopoulou, E., Lehander, M., Virding Culleton, S., Yang, W., Li, Y., Karpanen, T., Yoshizato, T., Rustad, E.H., Nielsen, M.M., Bollineni, R.C., et al. (2023). A T cell receptor targeting a recurrent driver mutation in FLT3 mediates elimination of primary human acute myeloid leukemia in vivo. Nat. Cancer *4*, 1474–1490. https://doi.org/10.1038/s43018-023-00642-8.

45. Marofi, F., Rahman, H.S., Al-Obaidi, Z.M.J., Jalil, A.T., Abdelbasset, W.K., Suksatan, W., Dorofeev, A.E., Shomali, N., Chartrand, M.S., Pathak, Y., et al. (2021). Novel CAR T therapy is a ray of hope in the treatment of seriously ill AML patients. Stem Cell Res. Ther. *12*, 465. https://doi.org/10.1186/s13287-021-02420-8.

46. Willier, S., Rothämel, P., Hastreiter, M., Wilhelm, J., Stenger, D., Blaeschke, F., Rohlfs, M., Kaeuferle, T., Schmid, I., Albert, M.H., et al. (2021). CLEC12A and CD33 coexpression as a preferential target for pediatric AML combinatorial immunotherapy. Blood *137*, 1037–1049. https://doi.org/10.1182/blood.2020006921.

47. Mehta, N.K., Pfluegler, M., Meetze, K., Li, B., Sindel, I., Vogt, F., Marklin, M., Heitmann, J.S., Kauer, J., Osburg, L., et al. (2022). A novel IgG-based FLT3xCD3 bispecific antibody for the treatment of AML and B-ALL. J. Immunother. Cancer *10*, e003882. https://doi.org/10.1136/jitc-2021-003882.

48. Radtke, S., Colonna, L., Perez, A.M., Hoffman, M., Kean, L.S., and Kiem, H.P. (2020). Isolation of a Highly Purified HSC-enriched CD34+CD90+CD45RA− Cell Subset for Allogeneic Transplantation in the Nonhuman Primate Large-animal Model. Transplant. Direct *6*, e579. https://doi.org/10.1097/TXD.0000000000001029.

49. Melenhorst, J.J., Chen, G.M., Wang, M., Porter, D.L., Chen, C., Collins, M.A., Gao, P., Bandyopadhyay, S., Sun, H., Zhao, Z., et al. (2022). Decade-long leukaemia remissions with persistence of CD4+ CAR T cells. Nature *602*, 503–509. https://doi.org/10.1038/s41586-021-04390-6.

50. Zhang, Y., Li, Y., Cao, W., Wang, F., Xie, X., Li, Y., Wang, X., Guo, R., Jiang, Z., and Guo, R. (2021). Single-Cell Analysis of Target Antigens of CAR-T Reveals a Potential Landscape of "On-Target, Off-Tumor Toxicity". Front. Immunol. *12*, 799206. https://doi.org/10.3389/fimmu.2021.799206.

51. Flugel, C.L., Majzner, R.G., Krenciute, G., Dotti, G., Riddell, S.R., Wagner, D.L., and Abou-El-Enein, M. (2022). Overcoming on-target, off-tumour toxicity of CAR T cell therapy for solid tumours. Nat. Rev. Clin. Oncol. *20*, 49–62. https://doi.org/10.1038/s41571-022-00704-3.

52. Santomasso, B.D., Park, J.H., Salloum, D., Riviere, I., Flynn, J., Mead, E., Halton, E., Wang, X., Senechal, B., Purdon, T., et al. (2018). Clinical and Biologic Correlates of Neurotoxicity Associated with CAR T Cell Therapy in Patients with B-cell Acute Lymphoblastic Leukemia (B-ALL). Cancer Discov. *8*, 958–971. https://doi.org/10.1158/2159-8290.cd-17-1319.

53. Frey, N.V., and Porter, D.L. (2016). Cytokine release syndrome with novel therapeutics for acute lymphoblastic leukemia. Hematology *2016*, 567–572. https://doi.org/10.1182/asheducation-2016.1.567.

54. Neelapu, S.S., Tummala, S., Kebriaei, P., Wierda, W., Gutierrez, C., Locke, F.L., Komanduri, K.V., Lin, Y., Jain, N., Daver, N., et al. (2018). Chimeric antigen receptor T-cell therapy - assessment and management of toxicities. Nat. Rev. Clin. Oncol. *15*, 47–62. https://doi.org/10.1038/nrclinonc.2017.148.

55. Sterner, R.C., and Sterner, R.M. (2021). CAR-T cell therapy: current limitations and potential strategies. Blood Cancer J. *11*, 69. https://doi.org/10.1038/s41408-021-00459-7.

56. AbbVie & Scripps-based Calibr Moves Novel 'Switchable' CAR-T Technology to Phase I Clinical Trial. https://www.trialsitenews.com/a/abbvie-scripps-based-calibr-moves-novel-switchable-car-t-technology-to-phase-i-clinical-trial.

57. Scripps Research. Calibr reports promising results from first-in-human clinical trial of switchable CAR-T (CLBR001 + SWI019), a next-generation universal CAR-T platform designed to enhance the versatility and safety of cell therapies. https://www.scripps.edu/news-and-events/press-room/2022/20220921-calibr-cart.html.

58. Ge, S.-S., Liu, S.-B., and Xue, S.-L. (2022). Developments and challenges of FLT3 inhibitors in acute myeloid leukemia. Front. Oncol. *12*, 996438. https://doi.org/10.3389/fonc.2022.996438.

59. Collados-Ros, A., Muro, M., and Legaz, I. (2024). Gemtuzumab Ozogamicin in Acute Myeloid Leukemia: Efficacy, Toxicity, and Resistance Mechanisms—A Systematic Review. Biomedicines *12*, 208. https://doi.org/10.3390/biomedicines12010208.

60. An, N., Wang, D., Zhang, P., Zhang, J., Parone, P., Hu, J., Bao, Y., Xu, L., Ruan, H., Wan, Y., et al. (2026). In vivo generation of anti-BCMA CAR-T cells in relapsed or refractory multiple myeloma: a phase 1 study. Nat. Med. *32*, 1257–1266. https://doi.org/10.1038/s41591-026-04244-6.

STAR★METHODS

KEY RESOURCES TABLE

REAGENT or RESOURCE	SOURCE	IDENTIFIER
Antibodies		
Anti-CD33 mouse monoclonal antibody (PE)	BioLegend	Cat# 303403; RRID: AB_314347
Anti-CD34 mouse monoclonal antibody (PE)	BioLegend	Cat# 343605; RRID: AB_1732033
CD135 (FLT-3/FLK-2) mouse anti-human Ab (PE)	Fisher Scientific	Cat# BDB558996; RRID: AB_397175
Anti-CD34 mouse monoclonal antibody (FITC)	BioLegend	Cat# 343503; RRID: AB_1731923
Anti-CD90 (Thy1) mouse monoclonal antibody (BV421)	BioLegend	Cat# 328121; RRID: AB_10933261
Anti-CD45RA mouse monoclonal antibody (AF700)	BioLegend	Cat# 304119; RRID: AB_493762
Anti-CD3 mouse monoclonal antibody (AF594)	BioLegend	Cat# 300446; RRID: AB_2563236
Cell Culture Reagents		
X-VIVO 15	Lonza	04-418Q
Human AB serum	Innovative Research	ISERAB100ML
StemSpan SFEM II	StemCell	19851
2-Mercaptoethanol	Thermo Fisher Scientific	21985023
IL-2	NCI BRB Preclinical Repository	N/A
Freestyle 293 Expression Medium	Fisher Scientific	12-338-026
DMEM	Corning	10–013
FBS	Thermo Fisher Scientific	10437028
Penicillin/streptomycin	Corning	30001CI
L-glutamine	Corning	25005CI
Sodium pyruvate	Lonza	13115E
Zeocin	Thermo Fisher Scientific	R25005
RPMI 1640	Cytvia	SH30027.LS
Bacterial and virus strains		
5-alpha Competent E. coli	NEB	C2987
Biological samples		
Anonymized whole peripheral blood collars	Boston Children's Blood Donor Center	N/A
Human BM $CD34^+$	StemCell	70002.2
Human CB $CD34^+$, Single source	StemCell	70008.4
Chemicals, peptides, and recombinant proteins		
ImmunoCult™ Human CD3/CD28 T cell Activator	STEMCELL	10971
RetroNectin® Recombinant Human Fibronectin Fragment	Takara Bio	T100B
Human FLT-3/CD135/FLK-2 Protein (His)	Sino Biological	10445-H08H-100
Human CD33/Siglec-3 Protein (His)	Sino Biological	12238-H08H-100
Human CD33/Siglec-3 Protein (His), Biotinylated	Sino Biological	12238-H08H-B-100
IVISbrite D-Luciferin Potassium Salt Bioluminescent Substrate	PerkinElmer	122799
Nano-Glo ® *In Vivo* Substrate, FFz	Promega	CS320501
PEG8000	Thermo Fisher Scientific	BP233-1
Sodium Chloride	Thermo Fisher Scientific	AAJ2161836
Dimethyl sulfoxide (DMSO), ACS reagent, >99.9%	Sigma-Aldrich	472301-1L
Invitrogen novex NuPAGE Sample Reducing Agent	Fisher Scientific	NP0009
Invitrogen novex NuPAGE LDS Sample Buffer	Fisher Scientific	NP0007
Invitrogen novex NuPAGE MOPS SDS Running Buffer	Fisher Scientific	NP0001
20X PBS Tween 20	Fisher Scientific	28352
Critical commercial assays		
RosetteSep™ Human T cell Enrichment	STEMCELL Technologies	15021

(*Continued on next page*)

Continued

REAGENT or RESOURCE	SOURCE	IDENTIFIER
CellTrace™ Violet Cell Proliferation Kit, for flow cytometry	Thermo Fisher Scientific	C34557
Human IFN-γ ELISA Set	BD Biosciences	555142
EZ-Link™ Sulfo-NHS-LC-Biotin, No-Weigh™ Format	Fisher Scientific	A39257
Octet® Streptavidin (SA) Biosensor	Sartorius	18–5019
Experimental models: Cell lines		
LENTI-X 293T	Takara Bio	632180
CD33$^+$ K562	Senti Biosciences	N/A
FLT3+ K562	Senti Biosciences	N/A
CD33$^+$ FLT3+ K562	Senti Biosciences	N/A
WT K562	Senti Biosciences	N/A
FLT3+ Nalm6	Senti Biosciences	N/A
Nalm6 (CD33 high)	ATCC	CRL-3273
MV4-11	ATCC	CRL-9591
THP-1	ATCC	TIB-202
Freestyle 293-F	Thermo Scientific	R79007
Jurkat T cells	Wong Lab	–
Experimental models: Organisms/strains		
Female NOD SCID NSG mice	Jackson Laboratories	005557
Recombinant DNA		
pHR-SFFV vector	Addgene	79121
pSecTag2A	–	–
Software and algorithms		
SpectraMax M5	Molecular Devices	N/A
FlowJo V10	TreeStar	N/A
Prism	GraphPad	N/A
BioRender	BioRender	N/A
Octet Analysis Studio 13.0	Sartorius	N/A
Other		
Octet RED384	FortéBio	OCTET RED 384

EXPERIMENTAL MODEL AND STUDY PARTICIPANT DETAILS

Source of primary human T cells

Anonymized whole peripheral blood was obtained from the Blood Donor Center at Boston Children's Hospital (Boston, MA) as approved by the University Institutional Review Board. Primary CD3$^+$ T Cells were isolated from blood using RosetteSep Human T cell Enrichment Cocktail (STEMCELL Technologies, 15021) according to the manufacturer's protocol then cryopreserved in 90% human AB serum (Innovative Research) and 10% DMSO.

Bone marrow derived human primary CD34 enriched cell were obtained as cryopreserved vials from STEMCELL Technologies.

Animals

Female NOD.Cg-Prkdscid Il2rgtm1Wjl/SzJ (NSG) mice, 6–8 weeks of age, were purchased from Jackson Laboratories (005557) and housed in the BUMC Animal Science Center for use in *in vivo* xenograft mouse experiments. All animal protocols were reviewed and approved by the Institutional Animal Care and Use Committee (IACUC) at Boston University (PROTP201800600). For all experiments, mice of the same sex were randomly assigned to experimental groups.

METHOD DETAILS

Cell line culture

HEK293T cells were cultured in complete DMEM (Corning) containing 10% FBS (Thermo Fisher), 100 units/mL penicillin (Corning), 100 μg/mL streptomycin (Corning), 1% L-glutamine (Corning), and 1 mM sodium pyruvate (Lonza). Jurkat T cells were cultured in complete RPMI (Cytvia) containing 5% FBS, 100 units/mL penicillin, 100 μg/mL streptomycin, and 1% L-glutamine. K562 cells,

MV4-11 cells, THP-1 cells, and Nalm6 cells were all cultured in complete RPMI containing 10% FBS, 100 units/mL penicillin, 100 μg/mL streptomycin, and 1% L-glutamine. Jurkat T cells, HEK293T cells, and K562 cells were not authenticated. Nalm-6, MV4-11, and THP-1 cell lines were obtained from ATCC, which performs STR profiling for cell line authentication prior to distribution. MOLM-13 cells were obtained from AddexBio, which also performs STR profiling for cell line authentication prior to distribution. Cells were used within 20 passages of receipt and were not further authenticated in-house. K562, MV4-11, and THP-1 cells were also assessed for CD33 and FLT3 expression by flow cytometry. All cell lines were regularly tested for mycoplasma contamination and confirmed mycoplasma-negative prior to use in co-culture assays or *in vivo* injection.

zipFv and zipCAR construct design

zipFvs were designed by Senti Biosciences as fusions of scFvs from known antibody clones (FLT3 clones NC-7 and D43, CD33 clones Hu195 and Mylotarg) to EE or JUN leucine zippers via a GC linker, followed by a 6X His tag for purification (Figure S1).

zipCARs were designed as previously described in the original SUPRA system as third generation CAR constructs expressed under an SFFV promoter in a lentiviral backbone (Figure S1). For the initial zipFv screening, both RR and JUN zipCARs were evaluated along with their cognate zipFv pairs. All zipCARs contained a myc tag c-terminal to the leucine zipper and were fused with mCherry after CD3z to assess expression levels.

Expression and purification of zipFv

For zipFv protein production, Freestyle 293-F cells (Thermo Scientific) were transfected with pSecTag2A mammalian expression vector based on the supplier's protocol. Three days post transfection, zipFv was collected from the cell supernatant through centrifugation at 400 x g for 5 min. The collected zipFvs were then purified by the Probond purification system with native conditions.

Western blot and SDS-PAGE gel electrophoresis

To verify the expression of zipFv proteins, western blot was performed based on standard protocol. Purified proteins were first mixed with NuPAGE LDS sample buffer (Fisher Scientific) and NuPAGE reducing agent (Fisher Scientific), and then heated on a thermocycler at 90°C for 10 min. Denatured samples were then loaded on SDS-PAGE gel in NuPAGE MOPS SDS running buffer (Thermo Scientific) and run at 200V for 30 min iBlot 2 gel transfer device was used to transfer protein to the membrane, which was then blocked by 5% of milk powder (Research Products International) in 1X PBS-Tween 20 (Thermo Scientific). To detect produced zipFvs, the blocked membrane was incubated overnight with 1:1000 diluted 6x-His Tag Monoclonal Antibody (4E3D10H2/E3) in PBS-Tween 20. Images were captured the next day using Gel Doc EZ imager (Biorad).

Primary human T cell isolation and culture

Primary $CD3^+$ T cells were isolated from anonymized whole peripheral blood obtained from Boston Children's Hospital using the STEMCELL RosetteSep Human T cell Enrichment Cocktail. After isolation, $CD3^+$ T cells were cryopreserved in 90% human Ab serum (Innovative Research) and 10% DMSO. For cell culture, complete T cell media consisted of X-VIVO 15 (Lonza) supplemented with 5% human Ab serum and 55 μM 2-mercaptoethanol. 50 units/mL of IL-2 (NCI BRB Preclinical Repository) was added to the media upon addition to the T cell culture.

Lentivirus generation and transduction of human T cells

Replication-incompetent lentivirus was packaged using HEK293T Lenti-X cells (Takara) and third generation lentiviral packaging and envelope plasmids. Briefly, HEK293T cells plated in a 125 mm^2 culture plate were PEI transfected with the lentiviral and zipCAR plasmids at 80–90% confluency. 24 h post transfection, HEK293T culture media was removed and replaced with FreeStyle 293 expression medium (Gibco) supplemented with 100 μg/mL streptomycin, 100 units/mL penicillin, 1 mM sodium pyruvate, and 5 mM sodium butyrate. Lentivirus-containing supernatant was collected two times between 48 and 96 h post transfection and replaced with fresh complete FreeStyle media between collections. The harvested lentivirus was concentrated using a 40% w/v PEG-8000 and 1.2 M NaCl solution overnight, then spun down for 1 h at 1600xg at 4°C. The supernatant was then poured off, and the viral pellet was resuspended in 4 mL cold PBS. Concentrated virus was either used immediately or flash frozen in liquid nitrogen and stored at −80°C.

T cells were thawed 48–72 h before transduction and cultured in complete X-VIVO 15 media for 24 h, then activated with Immunocult human CD3/CD28 T cell activator (STEMCELL) for up to 48 h. One day before transduction, a non-TC treated 6 or 12-well plate was coated with 20 μg/mL Retronectin (Takara) in PBS and incubated at 4°C overnight. The Retronectin solution was then removed, and the plate was blocked with 2% BSA solution for 30 min before adding 2 mL or 1 mL of concentrated virus per well for either a 6-well or 12-well transduction, respectively. This was spun down at 1200xg for 90 min, then removed and activated primary $CD3^+$ T cells were added at a concentration of 250k cells/mL and incubated at 37°C. Transduction efficiency was assessed as mCherry expression via flow cytometry, and transduced T cells were maintained between 500k and 1 mil cells/mL for 10–14 days for experimental use.

In-vitro NFAT Jurkat activation assay

On the day of transduction, 2 mL NFAT Jurkat cells were mixed with 50 μL of concentrated virus per well for a 6-well plate at a concentration of 250k cells/mL. The plate was spun down at 1000xg for 30 min then the virus containing media was replaced with fresh

Jurkat culture media by spinning down at 400xg for 5 min. Transduction efficiency was assessed by mCherry expression through flow cytometry 3 days after transduction. Transduced NFAT Jurkat cells were maintained between 250k and 1.5 mil cells/mL.

NFAT Jurkat activation assay was performed by incubating transduced NFAT-GFP Jurkat cells expressing zipCAR with engineered K562 target cells at an E:T ratio of 1:1 (100k NFAT Jurkat cells and 100k target cells) with 25 ng/well of each zipFv for 16–20 h at 37°C. Activation of NFAT Jurkat cells was assessed by NFAT-GFP expression through flow cytometry.

Antibody binding capacity assay

To quantitatively determine the levels of CD33 and FLT3 expressed on all target cell lines and human primary CD34 enriched cells, the Quantum MESF PE-conjugated kit from Bangs Laboratories was used. Briefly, the 5 bead populations provided in the kit (blank and 4 bead populations labeled with increasing amounts of PE) were run on the same day, in the same FACS buffer, and at the same fluorescence settings on the Attune NxT Flow Cytometer as triplicate samples of the cell lines stained with saturating quantities of anti-CD33 or anti-FLT3 PE-conjugated antibodies. Full width, half height gating around the histogram plots of each bead population was used to determine the mean fluorescence intensity (MFI) of each population. These MFIs were then used in the Bangs Laboratories' quantitative analysis template, QuickCal, to establish a calibration curve and calculate the molecules of equivalent fluorescence of each stained cell population. This value was divided by the fluorophore to protein ratio of the corresponding antibody to determine the antibody binding capacity per cell.

In-vitro cytotoxicity assays

Co-culture cytotoxicity assays were initially performed by incubating primary human $CD3^+$ T cells expressing zipCAR with engineered K562 target cells at an E:T ratio of 2:1 (50k CAR T cells and 25k target cells) along with a range of zipFv doses from 0 to 625 ng/well for 24 h at 37°C. Based on these initial assays, a dose of 125 ng of FLT3 zipFv and 25 ng of CD33 zipFv was used for subsequent assays that varied E:T ratio against K562, MV4-11, MOLM-13, and THP-1 cell lines. A similar dose response cytotoxicity assay method as follows for $FLT3^{high}$ and $CD33^{high}$ Nalm6 cell lines at an E:T ratio of 1:1 (25k CAR T cells and 25k target cells) with varying amounts of each zipFv from 0 to 325 ng/well. For all E:T variations in K562 cytotoxicity assays, a target cell number of 20k was used with CAR T amounts varying from 20k for a 1:1 ratio to 200k for a 10:1 ratio. For MV4-11, MOLM-13, THP1, and Nalm6 E:T cytotoxicity assays, a target cell number of 50k was used with CAR T amounts varying from 25k for a 1:2 ratio to 200k for a 4:1 ratio. Target cells were stained with either eFluor 450 or CellTrace Violet prior to co-culture, and after 24 h, the supernatant was saved at −80C for ELISA, and the cells were resuspended in FACS buffer to analyze via flow cytometry. Cytotoxicity was measured as viable target cell count compared to target cell only conditions by gating for eFluor 450+ or CellTrace Violet+ cells. In the mixed single positive K562 co-culture assay, $CD33^+$ K562 cells express GFP, allowing for specific gating based on the GFP signal. To characterize specific lysis, cytotoxicity assays included donor matched, mock transduced T cells incubated with the corresponding target cells at matched E:T ratios along with both zipFvs added as a negative control in addition to target only conditions.

Cytokine release assay

Supernatant was collected after co-culture for 24 h from cytotoxicity assays and frozen at −80°C for future analysis using an enzyme-linked immunosorbent assay (ELISA) to measure IFNγ secretion. The BD OptEIA Human IFNγ ELISA kit was used along with BD Reagent Set B according to the manufacturer's instructions. Supernatant was diluted at either a 1:50 or 1:100 ratio in assay diluent to ensure cytokine amounts were within the detection limits of the kit.

zipFv competition assay

To evaluate the potential competition between FLT3 and CD33 zipFvs when dosed simultaneously, co-culture assays were performed as previously described at an E:T ratio of 1:1 in a dose response matrix. Briefly, CAR T cells were cultured with one target cell type, either WT K562, $FLT3^{high}$ K562, or $CD33^{high}$ K562, along with varying doses of "targeting" and "non-targeting" zipFv from 0 to 625 ng/well such that at each dose of targeting zipFv, a range of non-targeting zipFv doses was added to evaluate interference. After 24 h of co-culture at 37°C, the supernatant was saved and analyzed via ELISA to measure IFNγ secretion as previously described.

Biolayer interferometry assay

CD33-biotin was purchased from Sino Biological, and FLT3-His was purchased (Sino Biological) and then biotinylated in-house using the EZ-Link Biotinylation kit (Fisher Scientific). After equilibrating tips in BLI buffer (1X PBS +0.05% Tween 20) and establishing a baseline, the streptavidin (SA) coated biosensor tips were dipped into wells containing 10 μg/mL of CD33 or FLT3 (separately) for immobilization, followed by transfer into the buffer to establish baseline 2. Loaded tips were then dipped into various concentrations of zipFv (0–1000 nM) to allow for association before transfer back into the buffer for dissociation. Analysis was performed in Octet Analysis Studio 13.0. Association was controlled by subtraction of a trace where the tip was not loaded with protein before exposure to zipFv, and dissociation was controlled via subtraction of a trace containing loaded protein but no exposure to zipFv. Y axis was aligned to the last 5 s of the second baseline, and data was fit to a Mass Transport model.

HSPC sparing assay

Bone marrow derived human primary CD34 enriched cells were obtained from StemCell and cultured in StemSpan SFEM II Human Hematopoietic Stem Cell Culture Medium (StemCell). Cells were thawed and stained for antigen expression then used in co-culture cytotoxicity assays within 24 h as described previously, with an E:T ratio of 2:1 and varying concentrations of each targeting zipFv. After 24 h of co-culture, the supernatant was saved, and cells were resuspended in FACS buffer for analysis via flow cytometry. Cytotoxicity was measured as viable $CD3^{-}CD34^{+}$ HSPC cell count compared to target cell only and zero zipFv conditions. HSC-enriched subset cytotoxicity was measured by further gating the HSPC population on $CD90^{+}$CD45RA-.

Xenograft mouse models

This study used only female NOD-scid IL2rgnull (NSG) mice to allow group housing and minimize injury from male aggression, as well as to reduce body-weight variability across cohorts. As such, the influence of host sex on tumor engraftment or CAR-T efficacy was not evaluated in this study. To obtain sex-independent results, a mix of male and female mice would be needed.

Cohorts of female NOD.Cg-Prkdcscid Il2rgtm1Wjl/SzJ (NSG) mice were ordered from the Jackson Laboratories and housed in the BUMC Animal Science Center. All animal protocols were reviewed and approved by the Institutional Animal Care and Use Committee (IACUC) at Boston University (PROTO201800600).

For the pilot Nalm6 dose determining experiment, NSG mice were injected with 500k luciferase-expressing Nalm6 cells intravenously on day 0. $CD33^{high}$ Nalm6 were engineered to express Antares luciferase while $FLT3^{high}$ Nalm6 were engineered to express Firefly luciferase for a dual reporter system. In animals containing both target cells, they were mixed at 250k each for a total cancer cell injection of 500k/mouse. On day 6, 5 million CAR-T cells were injected intravenously. For conditions containing zipFv, the first dose of zipFv was injected intraperitoneally on day 7 and every other day for a total of 4 doses. An intraperitoneal injection method was chosen to minimize injury to the tail vein due to frequent injections. Tumor burden was measured by IVIS Spectrum and was quantified as total flux (photons/sec) in the entire mouse. Images were acquired within 10 min of intraperitoneal injection of 150 mg/kg of D-luciferin (PerkinElmer) or 17.6 nM of FFz (Promega). Images were analyzed using Living Image (PerkinElmer).

For the final Nalm6 xenograft model, the dosing schedule was altered to inject CAR-T or Mock T cells on day 3, and 6 total doses of zipFv were administered including the initial dose incubated with the T cells 30 min prior to injection of T cells on Day 3.

For the MOLM-13 xenograft model, 250k engineered MOLM-13 cells expressing Firefly luciferase were injected into NSG mice intravenously on Day 0. 10 million CAR-T or mock T cells were also injected intravenously on Day 0. For conditions containing zipFv, the first dose was incubated with the CAR-T cells for 30 min prior to injections. Subsequently, zipFv was injected intraperitoneally every other day for a total of 8 doses. Tumor burden was measured by IVIS Spectrum and was quantified as total flux (photons/sec) in the entire mouse. Images were acquired within 10 min of intraperitoneal injection of 150 mg/kg of D-luciferin (PerkinElmer).

Statistical analysis

To evaluate statistical significance, data between groups were evaluated using an unpaired two-tailed *t* test. *p* values are reported (not significant = $p > 0.05$, * = $p < 0.05$, ** = $p < 0.01$, *** = $p < 0.001$), and error bars are plotted as standard deviations between replicates.